Two circadian oscillators in one cyanobacterium

Christin Köbler[a,1], Nicolas M. Schmelling[b,1], Alice Pawlowski[b,1], Philipp Spät[c], Nina M. Scheurer[a], Kim Sebastian[a], Lutz C. Berwanger[b], Boris Maček[c], Anika Wiegard[b], Ilka M. Axmann[b,*], Annegret Wilde[a,*]

[a]Institute of Biology III, Faculty of Biology, University of Freiburg, 79104 Freiburg, Germany; [b]Institute for Synthetic Microbiology, Biology Department, Heinrich Heine University Düsseldorf, 40225 Düsseldorf, Germany; [c]Department of Quantitative Proteomics, Interfaculty Institute for Cell Biology, Eberhard Karls University Tübingen, 72076 Tübingen, Germany

[1]C.K., N.M.S, and A.P. contributed equally to this study.

Corresponding authors:

*Prof. Dr. Annegret Wilde, Albert-Ludwigs-Universität Freiburg, Institut für Biologie III, Schänzlestr. 1, 79104 Freiburg, Germany, Phone: +49 (0) 761-20397828

*Prof. Dr. Ilka Axmann, Institute for Synthetic Microbiology, Biology Department, Heinrich Heine University Düsseldorf, 40225 Düsseldorf, Germany, Phone: +49 (0) 21181-10361

Email: annegret.wilde@biologie.uni-freiburg.de; Ilka.Axmann@hhu.de

Author Contributions: C.K., I.M.A. and A.W. designed the study. C.K., N.M.S., A.P., P.S., N.M.Sche., K.S., A. Wie, and L.B. performed and analyzed the experiments. All authors interpreted and discussed the data. C.K., N.M.S., A.P., P.S., B.M., A. Wie, I. M.A., and A.W. wrote the paper.

Competing Interest Statement: The authors declare no conflict of interest.

Keywords: cyanobacteria, circadian clock, *Synechocystis* 6803, KaiA

Abstract

Organisms from all kingdoms of life have evolved diverse mechanisms to address the predictable environmental changes resulting from the Earth's rotation. The circadian clock of cyanobacteria is a particularly simple and elegant example of a biological timing mechanism for predicting daily changes in the light environment. The three proteins KaiA, KaiB, and KaiC constitute the central timing mechanism that drives circadian oscillations in the cyanobacterium *Synechococcus elongatus* PCC 7942. In addition to the standard oscillator, *Synechocystis* sp. PCC 6803, another model organism for cyanobacterial research, harbors several divergent clock homologs. Here, we describe a potential new chimeric KaiA homolog that we named KaiA3. At the N-terminus, KaiA3 is similar to the NarL-type response regulator receiver domain. However, its similarity to canonical NarL transcription factors drastically decreases in the C-terminal domain, which resembles the circadian clock protein, KaiA. In line with this, we detected KaiA3-mediated stimulation of KaiC3 phosphorylation. Phosphorylation of KaiC3 was rhythmic over 48 h in vitro in the presence of KaiA3 and KaiB3 as well as in *Synechocystis* cells under free-running conditions after light/dark entrainment. This results in the presence of two different oscillators in a single-celled prokaryotic organism. Deletion of the *kaiA3* gene leads to KaiC3 dephosphorylation and results in growth defects during mixotrophic growth and in the dark. In summary, we suggest that KaiA3 is a nonstandard KaiA homolog, thereby extending the KaiB3-KaiC3 system in Cyanobacteria and potentially other prokaryotes.

Introduction

The three genes, *kaiA*, *kaiB,* and *kaiC,* encode the core circadian oscillator in Cyanobacteria[1]. Over the last few decades, the biochemical interplay between these three proteins has been studied in great detail in *Synechococcus elongatus* PCC 7942 (hereafter *Synechococcus*). The KaiC protein forms a homohexamer and has autokinase, autophosphatase, and ATPase activities[1, 2, 3, 4]. By associating with KaiC, KaiA stimulates the autokinase and ATPase activities of KaiC, and thus, the protein gets phosphorylated[5, 6, 7]. Upon phosphorylation of two neighboring residues (Ser431 and Thr432), KaiC undergoes structural rearrangements, exposing a binding site for KaiB[8, 9, 10]. After binding, KaiB sequesters KaiA from KaiC, promoting KaiC's autophosphatase activity, and the protein reverts back to its unphosphorylated state[8, 9, 11]. The interplay between KaiA and KaiB is crucial for the KaiC phosphorylation cycle, which confers clock phase and rhythmicity to the cell[12, 13]. For a more detailed review on the KaiABC oscillator and its regulatory network, see Cohen and Golden[14], Swan *et al*.[15] and Snijder and Axmann[16].

Although most studies on prokaryotic circadian rhythms have focused on the cyanobacterium *Synechococcus*, it has been shown that the standard KaiABC system is functionally conserved in other cyanobacteria[17]. However, in addition to the standard KaiABC system, divergent homologs of KaiB and KaiC have been identified in cyanobacteria, other bacterial species, and archaea[18]. The structure, mechanism of

function, and physiological roles of these homologs are often unclear. A few studies have demonstrated the role of KaiB and KaiC homologs in stress responses in e.g. *Legionella pneumophila*[19] and *Pseudomonas* species[20]. However, other Kai homologs are involved in the regulation of diurnal rhythms outside the cyanobacterial lineage. These include e.g. KaiB and KaiC homologs from the phototrophic bacterium *Rhodopseudomonas palustris*[21]. Recently, a KaiA-independent hourglass timer was reconstituted using *Rhodobacter sphaeroides* KaiC and KaiB homologs. *R. sphaeroides* KaiC exhibits a divergent extended C-terminus which is typically found in proteins belonging to the KaiC2 subgroup[22]. This C-terminal extension interacts with the protein, allowing for KaiA-independent phosphorylation. *R. sphaeroides* KaiB controls the phosphorylation-dephosphorylation cycle of KaiC depending on the ATP-to-ADP ratio, suggesting that metabolic changes during the day and night cycles drive this KaiBC clock[22].

The cyanobacterium *Synechocystis* sp. PCC 6803 (hereafter *Synechocystis*) is a facultative heterotrophic cyanobacterium that, in contrast to *Synechococcus*, can utilize glucose as an energy and carbon source. *Synechocystis* encodes, in addition to the canonical *kaiAB1C1* gene cluster, two further *kaiB* homologs, named *kaiB2* and *kaiB3*, and two *kaiC* homologs, named *kaiC2*, and *kaiC3*[23]. For the *Synechocystis* KaiB3-KaiC3 timing system, Aoki and Onai suggested a function in the fine-tuning of the core oscillator KaiAB1C1 by modulating its amplitude and period[24]. This idea was supported by Wiegard *et al.,* who investigated the characteristics of the KaiC3 protein and proposed an interplay between the KaiB3-KaiC3 system and the proteins of the standard clock system[25]. Furthermore, autophosphorylation and ATPase activities of *Synechocystis* KaiC3 have been verified, suggesting that enzymatic activities might be conserved across the KaiC protein family [25, 26, 27]. However, compared to *Synechococcus* KaiC, KaiC3 ATPase activity was reduced and lacked temperature compensation, an essential feature of true circadian oscillations[4, 25]. Recently, Zhao et al.[17] used a luminescence gene reporter to study circadian gene expression in the *Synechocystis* wild type in comparison to mutant strains lacking each of the *kai* genes. They demonstrated that the *kaiAB1C1* and *kaiB3C3* genes are both important for circadian rhythms in *Synechocystis,* whereas *kaiC2* and *kaiB2* deletion mutants still showed rhythmic gene expression, which is in agreement with previous suggestions by Aoki and Onai[24]. Phenotypic mutant analysis by our group revealed that two systems function in the autotrophy/heterotrophy switch, especially affecting heterotrophic growth. In contrast to the study by Zhao *et al.*[17], the deletion of *kaiC3* in the motile *Synechocystis* strain (PCC-M in[28]) used in our study had no effect on growth under light/dark cycles. However, the mutant strain displayed a growth defect under chemoheterotrophic conditions in the dark compared to the wild type[25, 29]. This impairment was less severe in comparison with the Δ*kaiAB1C1*-deficient strain, which completely lost its ability to grow in the dark. Notably, complete deletion of *kaiC2* was not possible in the wild-type strain used in our laboratory. Although Zhao et al.[17] clearly showed that deletion of the *kaiC3* and *kaiB3* genes affects the circadian rhythm of *Synechocystis*, it remains unclear whether the KaiB3-KaiC3 system can function as an oscillator. How can such a minimal system maintain circadian rhythmicity without KaiA? *Prochlorococcus* MED4, which lacks a *kaiA* gene in the entire genome, is suggested to

have no true circadian rhythmicity[30, 31]. Moreover, *Synechocystis* KaiC3 lacks the extended C-terminus, which is crucial for the oscillation of the *R. sphaeroides* KaiBC hourglass timer[22].

In *Synechococcus*, the KaiA protein functions as a homodimer and harbors two distinct domains connected by a linker sequence[32, 33, 34]. The N-terminal domain is similar to bacterial response regulators but lacks the aspartate residue crucial for phosphorylation; hence, it is designated as a pseudoreceiver domain (PsR domain)[32]. This domain was shown to bind the oxidized form of quinones and is therefore able to directly sense the onset of darkness and forward signals to the C-terminal domain[32, 35]. The C-terminus has a four-helix bundle secondary structure and is highly conserved within Cyanobacteria. The domain harbors the KaiA dimer interface and the KaiC binding site, and is necessary to stimulate the autophosphorylation activity of KaiC[32, 34]. Mutations in *kaiA*, resulting in altered periodicity, were mapped throughout both domains, indicating their importance for rhythmicity[34, 36].

To date, the regulatory network of the KaiB3-KaiC3 system in *Synechocystis* has remained enigmatic, as it does not interact with KaiA and does not utilize the SasA-RpaA output pathway, suggesting alternative yet unidentified components for KaiB3-KaiC3-based signal transduction[37]. In a large-scale protein-protein interaction screen, a potential interaction partner of KaiC3 was identified[38]. This protein, Sll0485, was categorized as a NarL-type response regulator and could be a potential element in the KaiB3-KaiC3 signaling pathway[39].

In this study, we computationally characterized Sll0485 and detected strong co-occurrences of the KaiB3-KaiC3 system with Sll0485 in the genomic context of Cyanobacteria and other bacteria. Bioinformatics analysis highlighted a resemblance between the N-terminal domain of the protein and the receiver domain of NarL-type response regulators, yet the C-terminal domain shared similarities with KaiA homologs. Therefore, we investigated the effects of Sll0485 on KaiC3 phosphorylation. Sll0485 increased the phosphorylation of KaiC3 *in vitro* and *in vivo*. We observed Sll0485-dependent 24-hour oscillations of KaiC3 phosphorylation in *Synechocystis* cells grown under light/dark and continuous light conditions. Those 24h oscillations of KaiC3 phosphorylation could be reconstituted *in vitro* by incubation with Sll0485 and KaiB3. Deletion of *sll0485* led to impaired viability during mixotrophic and heterotrophic growth, in line with previous studies on the KaiB3-KaiC3 system[25]. Thus, we propose that Sll0485 is a novel KaiA-like homolog linked to the KaiB3-KaiC3 system which together with the standard KaiA1B1C1 system controls circadian rhythms and the phototrophy-to-heterotrophy switch in *Synechocystis*.

Results

KaiA3 is a chimeric protein harboring a NarL-type response regulator domain at the N-terminus and a conserved KaiA-like motif at the C-terminus

151 The canonical clock genes, *kaiABC* and *kaiA1B1C1*, form a cluster in *Synechococcus* and
152 *Synechocystis*, respectively. In contrast, the *kaiB3* and *kaiC3* genes of *Synechocystis* are
153 localized in different regions of the chromosome (Fig. S1A). Here, the *kaiB3* gene forms a
154 transcriptional unit with the upstream open reading frame *sll0485.* Sll0485 has been
155 annotated as a NarL-type response regulator[39]. Using reciprocal BLAST analyses, we
156 detected orthologs of Sll0485 in 15 cyanobacterial species (16.5% of cyanobacterial
157 species contained at least one KaiC homolog), mainly belonging to the order
158 *Chroococcales*[40] (Data S1), and in five bacterial genera outside of Cyanobacteria, namely
159 *Roseiflexus*, *Chloroflexus*, *Chloroherpeton*, *Rhodospirillum*, and *Bradyrhizobium*.
160 Owing to the genetic context, we aligned the cyanobacterial Sll0485 orthologs with both,
161 a NarL-type response regulator (Fig. S2) and cyanobacterial KaiA proteins (Fig. 1A). The
162 canonical NarL protein consists of an N-terminal receiver domain, a linker, and a C-
163 terminal DNA-binding domain with a helix-turn-helix motif[39, 41]. The N-terminus of the
164 Sll0485 orthologs is conserved and indeed shows limited homology to NarL-type response
165 regulators (Fig. S2). However, the similarities to the NarL protein decreased in the C-
166 terminus (Fig. S2). Concurrently, conservation between Sll0845 and the KaiA protein
167 family increased (Fig. 1A). The conserved residues in the C-terminus correspond to
168 structurally important features of the *Synechococcus* KaiA protein, such as α-helical
169 secondary structures, the KaiA dimer interface, or residues critical for the KaiA-KaiC
170 interaction[32, 33] (Fig. 1A,). Additionally, the lack of conservation in the N-terminus
171 compared to that observed in known KaiA orthologs is consistent with the results of
172 Dvornyk and Mei, who proposed that different N-terminal domains exist for KaiA homologs
173 for functional diversification[42]. Because of its similarity to KaiA and synteny with the *kaiB3*
174 gene, we named the hypothetical Sll0485 protein KaiA3. Furthermore, to facilitate the
175 distinction of KaiA homologs, we will use the name KaiA1 for the *Synechocystis* KaiA core
176 clock homolog Slr0756.
177 The gene tree resulting from the multiple sequence alignment (Fig. 1A) distinctly separated
178 KaiA3 from canonical KaiA orthologs. To further investigate the evolutionary relationship
179 of KaiA3, multiple sequence alignments of the C-termini of orthologs of KaiA3, KaiA, and
180 Slr1783 (Rre1) as a reference for NarL orthologs in Cyanobacteria[43] were used to
181 construct a phylogenetic tree (Fig. S3). Here, KaiA3 orthologs form a distinct clade at the
182 basis of the KaiA orthologs when compared to both orthologous groups of Slr1783
183 (Rre1)/NarL (*E. coli*, UniProtKB - P0AF28) and KaiA simultaneously (Fig. S3). In summary,
184 these findings strengthen the idea that the C-terminus of KaiA3 functions similarly to that
185 of KaiA.

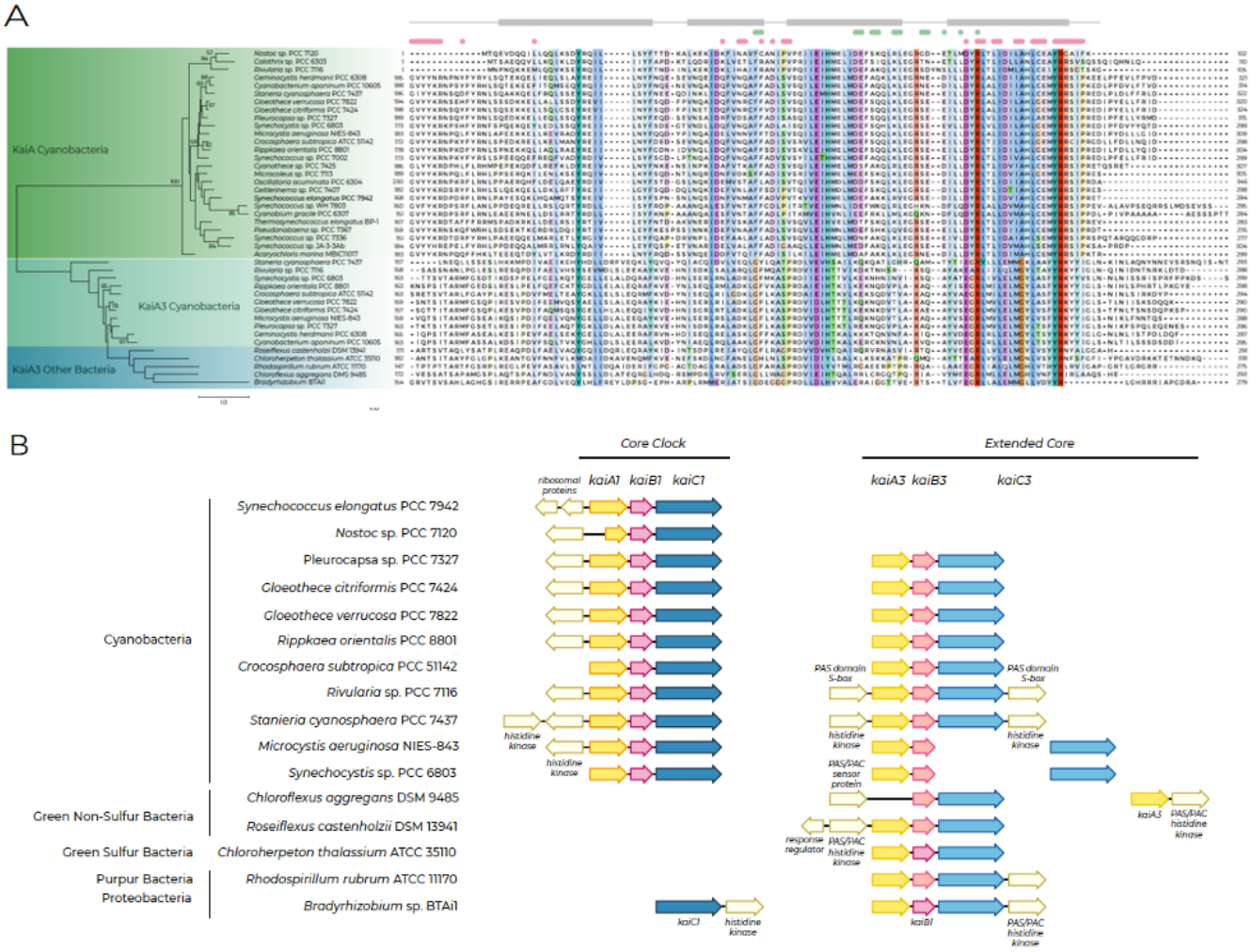
A
KaiA Cyanobacteria
KaiA3 Cyanobacteria
KaiA3 Other Bacteria
B
Core Clock
Extended Core
ribosomal proteins
kaiA1
kaiB1
kaiC1
kaiA3
kaiB3
kaiC3
Cyanobacteria
Synechococcus elongatus PCC 7942
Nostoc sp. PCC 7120
Pleurocapsa sp. PCC 7327
Gloeothece citriformis PCC 7424
Gloeothece verrucosa PCC 7822
Rippkaea orientalis PCC 8801
Crocosphaera subtropica PCC 51142
Rivularia sp. PCC 7116
Stanieria cyanosphaera PCC 7437
Microcystis aeruginosa NIES-843
Synechocystis sp. PCC 6803
Green Non-Sulfur Bacteria
Chloroflexus aggregans DSM 9485
Roseiflexus castenholzii DSM 13941
Green Sulfur Bacteria
Chloroherpeton thalassium ATCC 35110
Purpur Bacteria
Proteobacteria
Rhodospirillum rubrum ATCC 11170
Bradyrhizobium sp. BTAi1
PAS domain S-box
histidine kinase
PAS/PAC sensor protein
response regulator
PAS/PAC histidine kinase
C
RpaB
KaiC1
KaiB1
NhtA
CpmA
SasA
KaiA
KaiB2
RpaA
KaiC2
IrcA
LabA
LdpA
KaiB3
LalA
KaiA3
KaiC3
Pex
CikA
PrkE
CdpA
BH-Corrected P Value
10−3
10−5
10−7
10−9
10−11
10−13
10−15

186

Fig. 1. Bioinformatic analyses of Sll0485 (KaiA3). (A) Multiple sequence alignment and maximum likelihood-inferred phylogenetic reconstruction of KaiA3 and selected KaiA orthologs. The sequences were aligned with Mafft (L-INS-i default parameters, Jalview), trimmed to position 168 of the C-terminus of *Synechococcus* KaiA and are represented in the Clustalx color code with conservation visibility set to 25%. Marks above the alignment refer to *Synechococcus* KaiA as a reference. Light green bars and dots indicate residues critical for KaiC interaction, light pink bars and dots represent residues important for dimerization, and light gray blocks outline residues forming α-helices as secondary structures. Aligned sequences were used to infer a maximum likelihood protein tree. The scale bar indicates one substitution per position. Bootstrap values (n=1000) are displayed on the branches. Bootstrap values less than 50 are not shown. (B) Synteny analysis of *kaiA1B1C1* compared to *kaiA3*, *kaiB3*, and *kaiC3* genes for selected bacterial species. Analysis was performed with the online tool SyntTax, a prokaryotic synteny and taxonomy explorer (https://archaea.i2bc.paris-saclay.fr/synttax/; 2020-06-08). Default settings were used for analysis (best match, 10% norm. Blast). (C) Co-occurrence of KaiA3 using pairwise Fisher's exact test with circadian clock proteins in Cyanobacteria. Network of significant co-occurring circadian clock factors from Schmelling *et al.*[26], including KaiA3 in Cyanobacteria. The line color corresponds to the level of significance resulting from pairwise Fisher's exact test. Missing links were those with a p-value higher than 0.01. The node size is proportional to the degree of that node.

We further constructed three-dimensional models of KaiA3 to gain a better understanding of its potential functions. To date, no structure is available for KaiA3, and it is impossible to generate a reliable three-dimensional model covering the full-length KaiA3 sequence because of the enigmatic structure of the linker region, for which no significant similarities could be detected. However, secondary structure prediction suggested that the N-terminus structurally aligns with NarL (Fig. S4A). Therefore, we modeled the N-terminus (residues 1-140) and the remaining part of the sequence separately (residues 141-299). For the N-terminus, numerous hits for response regulator domains were obtained, with *E. coli* NarL (PDB 1A04) showing the highest degree of sequence similarity. The 3D-model structures of KaiA3 are highly similar and display the canonical fold of response regulator domains: a central five-stranded parallel β-sheet flanked on both faces by five amphipathic α-helices and a phosphorylatable aspartate residue in the β3-strand (Fig. S4B). This aspartate residue (D65) plays a role in response regulator phosphorylation (Fig. S2, blue stars) and is conserved in all species, except *Pleurocapsa* and *Microcystis*. Thus, most KaiA3 homologs, including the *Synechocystis* protein, harbor a potential phosphorylation site. Furthermore, the structure superimposes well on the PsR domain of KaiA, even though the PsR domain lacks the phosphate-accepting aspartate residue and the α4-helix between the β4- and β5-strands (Fig. S4B). The amino acid sequence between the β4- and β5-strands shows the least conservation between KaiA and KaiA3, yet the level of sequence conservation in this region is generally low for KaiA and its homologs[34]. In contrast to the N-terminal response regulator domain, the C-terminal domain of KaiA3 revealed a unique fold, which has only been detected in KaiA thus far[44], and the N-terminal domain of the phosphoserine phosphatase RsbU from *Bacillus subtilis*[45], namely, a unique four α-helix bundle constituting the KaiA-like motif (Fig. S4C). In conclusion, we propose that KaiA3 consists of two protein modules: i) the N-terminal domain, resembling a NarL-type response regulator receiver domain, including its phosphorylation site, and ii) the C-terminal domain displaying features of a KaiA-like motif. This is particularly intriguing

because putative *kaiA* orthologs outside Cyanobacteria have not been identified until recently[42].

Conserved synteny and co-occurrence of KaiA3 and the KaiB3-KaiC3 system among prokaryotes

As in *Synechocystis*, we found the *kaiA3* gene upstream of *kaiB3* in all the analyzed cyanobacterial genomes. Furthermore, the *kaiA3B3* cluster is usually extended by *kaiC3*, with only two exceptions (*Synechocystis* and *Microcystis aeruginosa* NIES-843), which resemble the structure of the canonical *kaiABC* gene cluster (Fig. 1B). Interestingly, *kaiA3B3C3* synteny was also found in other prokaryotic genomes that harbor orthologs of *kaiA3*, except for *Chloroflexus aggregans* DMS 9485 (Fig. 1B). Furthermore, we detected strong significant co-occurrences between KaiA3 and KaiB3 ($p<0.0001$) as well as between KaiA3 and KaiC3 ($p<0.0001$; Fig. 1C) in organisms encoding KaiC1. The co-occurrence of KaiB3 and KaiC3 has been previously shown[26]. Thus, KaiA3 forms a distinct set of proteins with KaiB3 and KaiC3, which show no further significant co-occurrence with other clock components (Fig. 1C,[26]). Altogether, both datasets suggest a functional relationship between KaiA3 and the KaiB3-KaiC3 system.

KaiA3 interacts with and promotes autokinase activity of KaiC3

Using yeast two-hybrid (YTH) experiments, we verified the interaction between the clock proteins KaiC3 and KaiA3 (Fig. 2A, Fig. S5), consistent with a previous large-scale protein-protein interaction analysis by Sato *et al*.[38]. Although KaiA3 clearly interacted with KaiC3, an interaction with KaiB3, the second element of the KaiB3-KaiC3 clock system, was not detected (Fig. S5B). This is not surprising, as it has been demonstrated that the interaction of the *Synechococcus* proteins KaiA and KaiB requires the presence of KaiC[46]. To further characterize the interaction of the proteins *in vitro*, we heterologously expressed different Kai proteins in *E. coli* and analyzed complex formation using clear-native PAGE (Fig. 2B and Fig. S6). The His-tagged KaiA3 protein (monomer: 35 kDa) migrated as a single band approximately 100 kDa in size, indicating the formation of KaiA3 homo-oligomers, at least dimers. *Synechococcus* KaiA migrated at ~60 kDa, in line with previous results[47], confirming the formation of KaiA dimers. The discrepancy in the migration pattern between KaiA3 (His-tagged) and KaiA (GST-tag removed) might be due to differences in their predicted charge (-19.17 for KaiA and -7.94 for KaiA3, respectively, at pH 7.0). Recombinant KaiB3 (monomer: 12 kDa) was shown to form monomers and tetramers after size exclusion chromatography[25]. KaiB3 displayed three distinct bands in the native gels (Fig. 2B). The two lower bands most likely represent the monomeric and tetrameric forms, whereas the uppermost band (~67 kDa) could be an impurity in the protein preparation. Recombinant KaiC3 was produced with an N-terminal Strep-tag[25]. Strep-tagged KaiC3 (monomer: 58 kDa) migrated as one band between 272 and 450 kDa and could represent a hexameric complex (348 kDa). Incubation of KaiC3 with KaiA3 alone led to protein accumulation in the wells in native PAGE, indicating precipitation of the

276 KaiA3/KaiC3 complex in the absence of KaiB3 (Fig. 2B). However, the interaction between
277 KaiA3 and KaiC3 was validated by immunoprecipitation-coupled liquid chromatography-
278 mass spectrometry (LC-MS) analysis of FLAG-tagged KaiC3 (Fig. S7). Furthermore, the
279 experiments did not reveal any interactions between KaiA3 and either KaiC1 or KaiC2
280 (Fig. S5, Fig. S7), indicating specificity of the KaiA3-KaiC3 interaction. No complex
281 formation was detected between KaiA3 and KaiB3 (Fig. 2B, Fig. S5 and Fig. S6). In
282 contrast, the formation of a large protein complex was observed when all three clock
283 components, KaiA3, KaiB3, and KaiC3, were incubated together for 16 h at 30°C (Fig. 2B;
284 Fig. S6). The size matches that of a complex consisting of one KaiC3 hexamer, six KaiA3
285 dimers, and six KaiB3 monomers (840 kDa). The presence of KaiA3 in the complex was
286 validated by western blot analysis using an anti-His antibody (Fig. 2B, Fig. S6). As
287 expected, no such complex was formed when KaiA3 was replaced with *Synechococcus*
288 KaiA (Fig. 2B). Moreover, no such complex was formed when KaiB3 was replaced by its
289 isoform KaiB1, suggesting that KaiB3 is specific for KaiA3 as well and that KaiB3 might
290 recruit KaiA3 to the KaiC3/KaiB3 complex (Fig. S6).

291 Previous studies have shown that KaiC3 has autokinase activity, which is independent of
292 KaiA1[25, 27]. Since our studies revealed an interaction between KaiC3 and KaiA3, we were
293 interested in probing the influence of KaiA3 on the phosphorylation of KaiC3. The
294 recombinant Kai proteins described above were used for this purpose. KaiC3 was
295 incubated for 16 h at 30°C in the presence or absence of other Kai proteins, and its
296 phosphorylation state was analyzed by SDS-PAGE (Fig. 2C), and LC-MS/MS (Fig. S8).
297 Since KaiC3 was partially phosphorylated after purification from *E. coli,* the protein
298 preparation was incubated for 18 h at 30°C prior to the start of the assays. During this
299 incubation period, KaiC3 autodephosphorylated, as is typical for KaiC proteins (Fig. 2C,
300 NP-KaiC3)[44]. Addition of KaiA3 led to phosphorylation of KaiC3, while the presence of
301 *Synechococcus* KaiA had no influence on the phosphorylation state of KaiC3. In contrast,
302 KaiC3 dephosphorylation was enhanced by KaiB3 (Fig. 2C, upper panel). Replacing
303 KaiB3 with its isoform, KaiB1, in samples containing KaiA3, maintained KaiC3 in the
304 phosphorylated state (Fig. 2C, lower panel). Analysis of KaiC3 phosphorylation by LC-
305 MS/MS- identified the neighboring residues Ser423 and Thr424 as phosphorylation sites,
306 which are conserved across KaiC homologs (Fig. S8). Based on these analyses, we
307 conclude that KaiA3 likely has a KaiA-like function in promoting the phosphorylation of
308 KaiC3. Neither *Synechococcus* KaiA nor *Synechocystis* KaiB1 could substitute for KaiA3
309 or KaiB3, respectively, demonstrating that the *Synechocystis* KaiA3/KaiB3/KaiC3 proteins
310 represent a separate functional complex. Only KaiA3 stimulated the autokinase activity of
311 KaiC3, which in turn promoted its interaction with KaiB3. Interaction with KaiB3, but not
312 KaiB1, enhances the dephosphorylation of KaiC3.

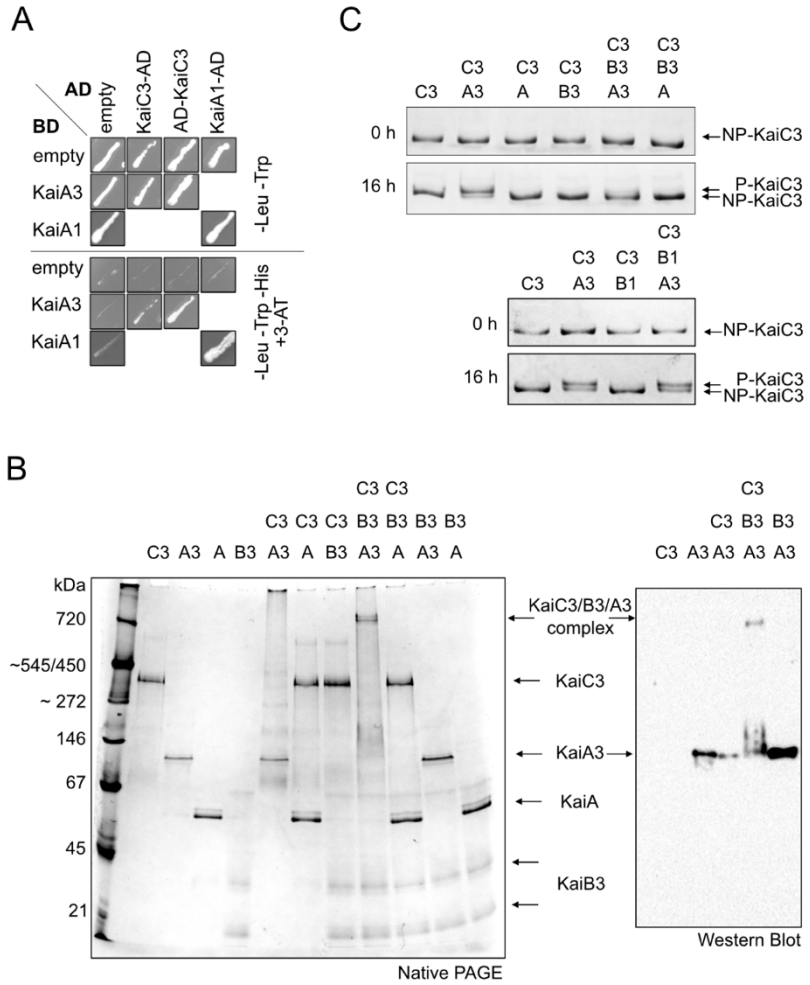

Fig. 2. Analysis of KaiA3 protein interactions and KaiC3 phosphorylation. (A) YTH interaction analysis of KaiA3 with KaiC3. The KaiA1 dimer interaction was used as a positive control. YTH reporter strains carrying the respective bait and prey plasmids were selected by plating on complete supplement medium (CSM) lacking leucine and tryptophan (-Leu -Trp). AD, GAL4 activation domain; BD, GAL4 DNA-binding domain; empty, bait, and prey plasmids without protein sequence (only AD/BD domain). The physical interaction between bait and prey fusion proteins was determined by growth on complete medium lacking leucine, tryptophan, and histidine (-Leu -Trp -His) and the addition of 12.5 mM 3-amino-1,2,4-triazole (3-AT). The BD was fused to the N-terminus of KaiA3. For a clear presentation, spots were assembled from several replicate assays (original scans are shown in Fig. S5). (B) Interaction analysis of the recombinant Kai proteins on native polyacrylamide gels. Proteins were incubated for 16 h at 30°C and subsequently subjected to 4-16% clear native PAGE. Gels were either stained with Coomassie Blue (left side) or blotted and immunodecorated with a monoclonal anti-His antibody to detect recombinant KaiA3-His6 (right side). Recombinant *Synechococcus* KaiA was used for comparison. (C) KaiC3 phosphorylation depends on the presence of KaiA3 and KaiB3. KaiC3 was dephosphorylated by incubating for 18 h at 30°C prior to the start of the assay (NP-KaiC3). 0.2 µg/µl NP-KaiC3 was incubated at 30°C in the presence or absence of 0.1 µg/µl *Synechocystis* KaiA3, KaiB3 and KaiB1 and *Synechococcus* KaiA, respectively. Aliquots were taken at 0 h and 16 h, followed by separation on a high-resolution LowC SDS-PAGE gel in Tris-Tricine buffer and staining with Coomassie blue. A slow-migrating band representing the phosphorylated form of KaiC3 (P-KaiC3) was observed only in the presence of KaiA3.

335 *KaiC3 phosphorylation oscillates in vitro and in* Synechocystis *cells*
336
337 The opposing effects of KaiA3 and KaiB3 on KaiC3 phosphorylation imply that these three
338 *Synechocystis* proteins may form a functional *in vitro* oscillator. We monitored the
339 phosphorylation of KaiC3 in concert with KaiB3 and various concentrations of KaiA3 over
340 a period of 48 h (Fig. 3A, B; Fig. S9). In the presence of 1.4 μM and 2.8 μM KaiA3
341 (corresponding to a ~1:1.2 and 1:2.4 stoichiometry of KaiA3:KaiC3), we could reconstitute
342 ~24h oscillations in KaiC3 phosphorylation (Fig. 3A, B; Fig. S9). Compared to the
343 *Synechococcus* KaiABC oscillator[48, 49], lower KaiA3 concentrations failed to generate
344 oscillations and the protein was mainly dephosphorylated. The stimulating effect of KaiA3
345 on KaiC3 phosphorylation was saturated at a KaiA3 concentration of 4.2 μM, which
346 corresponds to a KaiA3:KaiC3 stoichiometry of 1:0.8. Hence, the KaiC3 oscillations were
347 clearly dependent on the KaiA3 concentration.
348 To evaluate whether the self-sustained KaiC3 phosphorylation rhythms detected above
349 are also present in *Synechocystis* cells and are diurnal or circadian in nature, we grew
350 cells in a light/dark cycle, followed by constant illumination. We separated whole-cell
351 extracts on a Phostag gel and identified KaiC3 by Western blot analysis (Fig. 3C) using a
352 KaiC3-specific antibody[27]. We detected 4-5 bands which partially overlapped or were
353 slightly shifted in comparison to the bands detected in the Δ*kaiC3* strain. It seems that
354 there is some cross-reaction with KaiC1, KaiC2 or another protein The two prominent
355 bands indicated in Fig. 3C and which are absent in the Δ*kaiC3* strain most probably reflect
356 two different phosphorylation states of KaiC3. Based on the in vitro data with the isolated
357 Kai proteins and their similar migration patterns in Phos-tag SDS-PAGE analysis
358 compared to the whole cell extract (Fig. S9C), we suppose that the very upper (red arrow)
359 and one of the lower bands (blue arrow) in Fig. 3C represent the fully phosphorylated and
360 non-phosphorylated forms of KaiC3, respectively. In the Δ*kaiA3* mutant, the lowest band
361 was mainly present, indicating that KaiC3 was mostly dephosphorylated in this strain.
362 Incubation of KaiC3 with Lambda phosphatase resulted in comparable accumulation of
363 the lower band (Fig. S9D). In contrast, in the KaiA3 overexpression strain, KaiC3 was
364 highly phosphorylated in comparison to the wild type (Fig. 3C). In addition, two or more
365 bands were detected in the in vitro assays, as well as in the cell extracts (Fig. 3B, C; Fig.
366 S9C) which partly overlapped with an unspecific band detected in the Δ*kaiC3* strain in
367 Phos-tag SDS-PAGE analysis. These bands might reflect single phosphorylated states of
368 KaiC3. In summary, our in vitro and in vivo data demonstrate that KaiC3 phosphorylation
369 strongly depended on KaiA3. Furthermore, KaiC3 phosphorylation showed sustained
370 oscillations with a 24 hours rhythm in *Synechocystis*, hence displaying a characteristic
371 feature of a circadian oscillator.

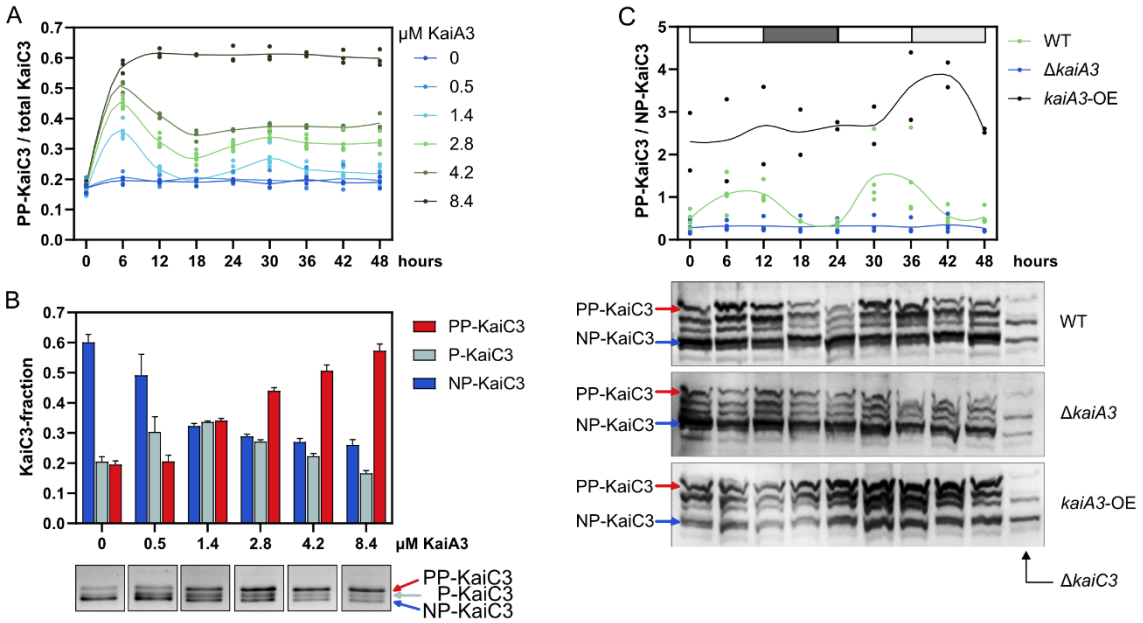

Fig. 3. Analysis of KaiA3-dependent KaiC3 phosphorylation. (A) KaiC3 (3.4 μM) was incubated with KaiB3 (7.4 μM) and various concentrations of KaiA3 at 30°C. Aliquots incubated for the indicated time periods were applied to a high-resolution LowC SDS-PAGE gel, proteins were separated in Tris-glycine buffer, and the relative band densities of the different KaiC3 phosphorylation states: unphosphorylated (NP), single-phosphorylated (P), and double-phosphorylated (PP) were estimated densitometrically. (A) *In vitro* ratio of fully phosphorylated KaiC3 (PP-KaiC3) to total KaiC3 at various concentrations of KaiA3. Dots display replicates (n=3); the line represents an akima spline curve. Assays with 1.4 μM KaiA3 and 2.8 μM KaiA3 were each analyzed twice on the gel, resulting in 6 replicates in total. Representative gels from each assay are shown in Fig. S9A. (B) Detailed analysis of KaiC3 phosphorylation after 6h of incubation with different KaiA3 concentrations. The fractions of double (PP), single (P), and unphosphorylated KaiC (NP-KaiC3) are plotted as average +SD from the three assays, also shown in A. Below the graph, representative band patterns are shown (assembled from Fig. S9A). (C) The ratio of fully phosphorylated KaiC3 (PP-KaiC3) to non-phosphorylated KaiC3 (NP-KaiC3) in *Synechocystis* wild-type, *kaiA3* mutant (Δ*kaiA3*), and *kaiA3* overexpression (*kaiA3-OE*) strains (Fig. S1). Whole cell extracts were separated using Phos-tag SDS-PAGE and immunodecorated with a KaiC3-specific antiserum. Samples were collected every 6 h from cells grown in a 12-h light/dark cycle, followed by constant light. The white and dark gray boxes represent light and dark periods, respectively, and the light gray box represents the subjective night. Representative blots are shown. Whole cell extracts from the *Synechocystis* Δ*kaiC3* mutant (12 h time point) were used as a control. Dots in the graph display the replicates (n=2-3); the line represents an akima spline curve. Plots were generated using GraphPad Prism, version 9.5.1.

397 *Deletion of kaiA3 impacts growth and viability during mixotrophic and chemoheterotrophic*
398 *growth*
399
400 What is the function of this additional Kai protein oscillator in *Synechocystis*? In our
401 laboratory, deletion of *kaiC3* led to growth impairment in complete darkness on glucose,
402 but not in light/dark cycles[25]; thus, the *kaiA3* knockout mutant (Δ*kaiA3*) was analyzed
403 under various growth conditions. The cells were grown in liquid culture under constant
404 light, plated on agar at different dilutions, and grown photoautotrophically (Fig. 4A) and
405 photomixotrophically (Fig. 4B) under continuous light and 12-h light/12-h dark cycles or
406 chemoheterotrophically (Fig. 4C). Because the strains grew very slowly under
407 chemoheterotrophic conditions, the cells were spotted at higher concentrations under
408 these conditions. There were no differences in the viability of the mutant strains in
409 comparison to that of the wild type under photoautotrophic conditions in continuous light
410 and light/dark cycles. Under photomixotrophic conditions, the Δ*kaiA3* strain showed less
411 viability, which was partly restored by re-insertion of *kaiA3*. It appears that the amount of
412 KaiA3 is critical for the function of the system, which is consistent with our data on KaiA3-
413 dependent KaiC3 phosphorylation (Fig. 3). Surprisingly, the mutant strain lacking all three
414 alternative *kai* genes (Δ*kaiA3B3C3)* exhibited a different growth phenotype under
415 photomixotrophic conditions. In light/dark cycles, this strain grew well and seemed to have
416 some advantages in comparison to the wild type (Fig. 4B). Spot assays under
417 chemoheterotrophic conditions provided a clearer picture; the mutant strain lacking *kaiA3*
418 and the triple knockout showed a similar phenotype. They were unable to grow in complete
419 darkness, and this ability was fully restored in the complementation strain (Fig. 4C). These
420 results coincide with previously detected impairments displayed by the Δ*kaiC3* strain
421 during chemoheterotrophic growth[25], strengthening the idea that the non-standard KaiA3-
422 KaiB3-KaiC3 system is a regulatory complex with the same function.

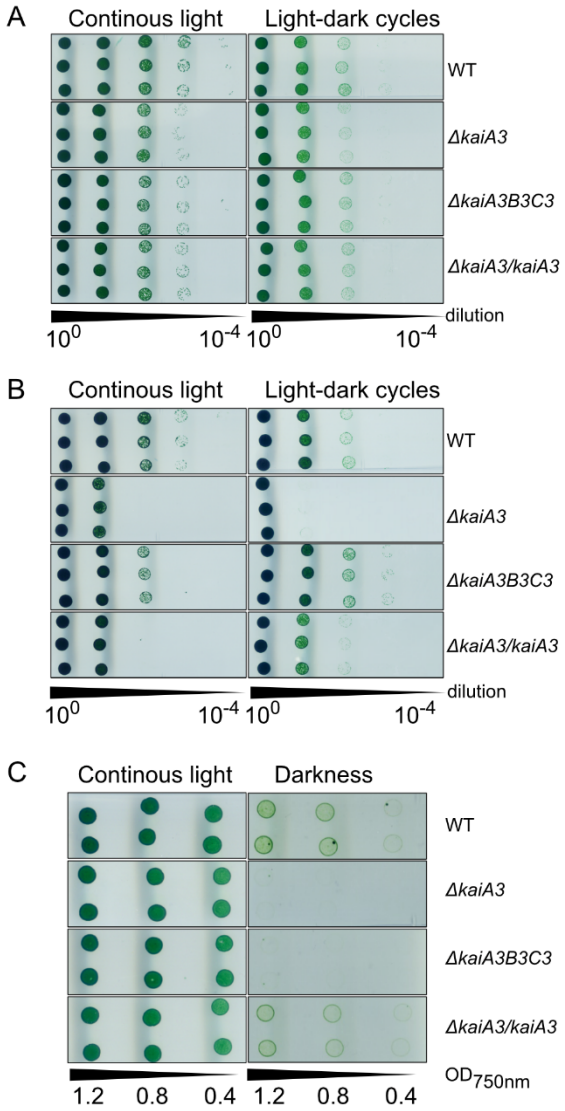

Fig. 4. Deletion of *kaiA3* results in growth defects during mixotrophic and chemoheterotrophic growth. Proliferation of the wild type (WT), the Δ*kaiA3* and Δ*kaiA3B3C3* deletion mutants, and the Δ*kaiA3*/*kaiA3* complementation strain was tested under (A) phototrophic (continuous light, - glucose), (B) photomixotrophic (continuous light, + glucose), and (C) heterotrophic (darkness, + glucose) conditions. Strains were grown in liquid culture under constant light, and different dilutions were spotted on agar plates and incubated under the indicated light conditions with a light phase corresponding to 75 µmol photons m^{-2} s^{-1} white light. Representative result from three independent experiments are shown. (A) Cultures were diluted to an OD_{750nm} value of 0.4, and tenfold dilution series were spotted on agar plates. Plates were analyzed after 6 or 8 days of continuous light and 12h/12h light/dark cycles, respectively. (B) Same as (A), but the cells were spotted on agar plates containing 0.2 % glucose. (C) Cultures were diluted to OD_{750nm} values of 1.2, 0.8, and 0.4, and spotted on agar plates supplemented with 0.2% glucose. The plates were analyzed after 3 and 26 d of continuous light and darkness, respectively.

Discussion

Our knowledge of the function, composition, and network of clock systems in prokaryotes, including cyanobacteria, is increasing steadily. Even though multiple copies of the core clock proteins KaiB and KaiC are encoded in bacterial genomes, the canonical KaiA was found only as a single copy in Cyanobacteria yet[26, 27, 42, 50]. By identifying a chimeric KaiA3 and verifying its interaction with the KaiB3-KaiC3 complex, we added another component to the diversity of bacterial clock systems.

KaiA-like proteins outside of Cyanobacteria and primordial clocks

In addition to KaiA3, new putative KaiA orthologs have been bioinformatically identified in prokaryotes outside Cyanobacteria[42]. Therefore, we suggest that such proteins may play a previously overlooked role in KaiB-KaiC-based systems. Exploring this possibility could provide valuable insights into unanswered research questions, such as the mechanism responsible for the rhythmic processes observed in *Rhodospirillum rubrum.* Indeed, this purple bacterium lacks KaiB1 and KaiC1 orthologs but possesses KaiA3, KaiB3, and KaiC3 (53) (Figure 1). Notably, the recently described oscillator from *Rhodobacter sphaeroides* (*Rhodobacter*), which consists of homologs of KaiC2 and KaiB2, can form an hourglass timer. This primordal *Rhodobacter* clock can function without KaiA. However, the *Rhodobacter* KaiB2-KaiC2 system requires an environmental signal to reset the clock[22]. A similar primordial clock has been suggested to be present in *Rhodopseudomonas palustris*[21] and the cyanobacterium *Prochlorococcus* MED4[30, 31]. However, other bacterial KaiB and KaiC homologs, including the KaiC2-KaiB2 system from *Synechocystis*, are believed to have clock-independent functions[17, 51, 52].
It has been proposed that *kaiC* is the oldest evolutionary member of circadian clock genes[50]. KaiC homologs can be found even in Archaea where it was found to control e. g. motility of *Sulfolobus acidocaldarius* by protein interaction[53]. The later addition of KaiB was enough to form a primordial timekeeper which needs a signal for daily resetting of the clock[21, 22, 30, 31]. In *Rhodobacter* KaiC2, dephosphorylation is regulated by the stability of coiled-coil interactions between two connected hexamers as well as by KaiB[22]. However, whether autophosphorylation or dephosphorylation dominates depends primarily on the ATP/ADP ratio. Hence, the KaiC2-KaiB2 timer cannot oscillate autonomously but responds to changing ATP/ADP levels. Therefore, it was suggested that the *Rhodobacter* clock represents an ancient timer that depends on changes in photosynthetic activity during the day-night switch[22].
With the evolution of KaiA, a self-sustained oscillator was developed that allowed for true circadian oscillations in gene expression, which can be observed in cyanobacteria. Why does KaiC require KaiA to drive persistent oscillations? By default, the A-loops of *Synechococcus* KaiC hexamers adopt a buried conformation, which inhibits autophosphorylation. Only the binding of KaiA favors phosphorylation by stabilizing A-loop exposure[5]. In contrast, *Rhodobacter* KaiC2 constantly exposes its A-loops, sterically allowing high intrinsic phosphorylation[22].

482 The interacting residues between KaiA and KaiC are less conserved in both *Synechocystis*
483 KaiA3 and KaiC3[27, 54] (Fig. 1). Since we demonstrated an interaction between KaiC3 and
484 KaiA3, it is likely that co-evolution of the two proteins occurred. Another remarkable feature
485 of *Rhodobacter* KaiC2 is that the latter displays an extended C-terminus that connects two
486 hexamers via coiled-coil interactions to adopt a homododecamer instead of a typical
487 hexamer[22, 55]. KaiC3 does not have such an extended C-terminus[27], and we only observed
488 the formation of hexamers or smaller oligomers[25] (Fig. 2).
489
490 *The two-domain architecture of KaiA3 and complex formation*
491
492 KaiA3 formed a distinct clade at the basis of the KaiA clade. Apart from its presence in the
493 N-terminal domain of phosphatase RsbU of *Bacillus subtilis*, a distinctive structure of the
494 KaiA C-terminus has rarely been observed[45]. RsbU acts as a positive regulator of the
495 alternative sigma factor B, which is involved in the general stress response[56]. The N-
496 terminal domain of RsbU forms dimers similar to KaiA, and the proposed binding site for
497 its corresponding activator, RsbT, is in an equivalent location to the KaiC-binding site on
498 KaiA[45]. These findings may reflect how protein domains change during evolution, while
499 their original functions are conserved. However, a link between RsbU and the recently
500 proposed circadian clock in *Bacillus subtilis* has not yet been identified[57]. Moreover,
501 circadian rhythms have been observed in several prokaryotes that do not encode Kai
502 orthologs, suggesting the convergent evolution of circadian rhythms in prokaryotes[57, 58].
503 Further in-depth analyses are needed to elucidate whether KaiA3, together with KaiB3
504 and KaiC3, or the well-studied *Synechococcus* circadian clock present a more ancestral
505 system, because analysis of a larger dataset recently suggested that the canonical *kaiA*
506 gene evolved at the same time as cyanobacteria[42].
507 Taken together, these data are consistent with a model in which KaiA3 can fulfill the
508 functions of a true KaiA homolog, such as dimerization, binding to KaiC3, and enhancing
509 KaiC3 autophosphorylation. Other mechanistic processes, such as sequestration to the
510 CI ring by binding to KaiB3, remain to be investigated but are clearly possible. By mixing
511 KaiA3, KaiB3, and KaiC3, we reconstituted a *bona fide in vitro* oscillator (Fig 3A),
512 suggesting that the observed in vivo oscillation of KaiC3 phosphorylation can run
513 independently of the KaiA1B1C1 clock, and that the amount of KaiA3 is critical for the
514 phosphorylation rhythm.
515 The *Rhodobacter* hourglass-like timer requires environmental cues for daily resetting.
516 However, entrainment by metabolites has also been described for more elaborate, true
517 circadian oscillators. In addition to entrainment by the input kinase CikA[59], the
518 *Synechococcus* clock can be entrained directly by the ATP/ADP ratio and oxidized
519 quinones[35, 60]. Moreover, CikA does not sense light directly but perceives the redox state
520 of the plastoquinone pool[61, 62]. In addition, glucose feeding can entrain *Synechococcus*
521 when engineered to take up glucose[63]. In plants, it has been demonstrated that both
522 exogenous sugars and internal sugar rhythms resulting from cyclic photosynthetic activity
523 entrain the clock[64]. *Synechocystis* can naturally utilize glucose, which may make it even
524 more susceptible to metabolic entrainment by sugars. Notably, the *Synechocystis* wild-

525 type strain used in this study was able to grow in complete darkness when supplemented
526 with glucose. This is different from an earlier study that showed that *Synechocystis* needs
527 a 5 min blue-light pulse at least once a day to grow heterotrophically in the dark[65]. The
528 authors described this behavior as light-activated heterotrophic growth. There are no
529 studies that explain why cells require this short light pulse, but it is also clear that our
530 laboratory strain grows fully chemoheterotrophically[29].
531 In contrast to *Synechococcus*, CikA from *Synechocystis* is a true photoreceptor that binds
532 a chromophore[66]. Thus, it remains unclear whether CikA has a similar function in both
533 cyanobacteria, and whether it interacts with both circadian clock systems in
534 *Synechocystis*. The high structural similarity of the N-terminal domain of KaiA3 to
535 response regulator domains from other organisms indicates that the core structure and
536 activity are maintained, while adaptivity and variation provide specificity for acting in
537 distinct pathways[24]. Within KaiA3, the aspartate residue crucial for phosphorylation is
538 conserved. Theoretically, the protein could receive an input signal from a cognate histidine
539 kinase, which has not yet been identified. Thus, there are potentially important differences
540 related to input and output factors, and possibly entrainment of different cyanobacterial
541 circadian clock systems.
542
543 *The function of KaiA3 in Synechocystis*
544
545 The physiological function of the KaiA3-KaiB3-KaiC3 clock system seems to be related to
546 the different metabolic modes of *Synechocystis.* Mutants deficient in *kaiA3* lose the ability
547 to grow chemoheterotrophically on glucose, which is an aggravated effect compared to
548 *kaiC3*-deficient mutants, which merely show reduced growth rates during heterotrophy[25].
549 Similarly, in *Synechococcus,* the disruption of *kaiA* led to one of the most severe effects
550 on activity loss and was traced back to the unbalanced output signaling of the circadian
551 clock[67]. The overaccumulation of KaiA3 also appeared to disturb the system (Fig. S10).
552 Such an effect was also shown for the *Synechococcus* clock system, in which increased
553 KaiA levels promote the hyperphosphorylation of KaiC[6, 68], thereby deactivating rhythmic
554 gene expression[69]. Surprisingly, inactivation of the complete KaiA3-KaiB3-KaiC3 system
555 resulted in a different phenotype. While growth in darkness on glucose was strongly
556 affected, similar to the single mutants, photomixotrophic growth was even slightly better
557 in the *kaiA3B3C3* strain compared to the wild type. It is possible that in the absence of
558 KaiA3, the altered interaction of KaiC3 with KaiC1 leads to aggravated growth defects in
559 the Δ*kaiA3* mutant. However, when a complete oscillator is missing, the KaiA1B1C1
560 oscillator can compensate for this under certain growth conditions.
561 In *Synechocystis*, Δ*kaiA3*-like phenotypes, such as impaired viability during light/dark
562 cycles or complete loss of chemoheterotrophic growth on glucose, were also observed for
563 Δ*kaiA1B1C1*, Δ*sasA*, and Δ*rpaA* mutants[29, 70]. For Δ*sasA,* it was shown that the mutant
564 strain was able to accumulate glycogen but was unable to utilize the storage compound
565 to grow heterotrophically, probably because of its inability to catabolize glucose[70]. A recent
566 metabolomics study suggested that the growth inhibition of Δ*kaiA1B1C1* and Δ*rpaA*
567 mutants in a light/dark cycle might be at least partly related to a defect in the inhibition of

568 the RuBisCo enzyme in the dark and increased photorespiration, leading to the
569 accumulation of the potentially toxic product 2-phosphoglycolate[71]. This previous study
570 also revealed an enhanced growth defect in Δ*kaiA1B1C1* and Δ*rpaA* mutants under
571 photomixotrophic conditions in light/dark cycles, similar to the Δ*kaiA3* strain in the current
572 study. This further supports the idea that one of the functions of the KaiA3-B3-C3 system
573 is to fine-tune the core clock system, KaiA1B1C1. Clearly, there is a difference in the
574 phenotypes between our study and the results demonstrated by Zhao et al.[17], who
575 analyzed single and double *kaiB3* and *kaiC3* knockout strains. In light/dark cycles, the
576 *kaiB3C3* knockout strain showed a reduced growth rate compared to the wild-type control
577 under photoautotrophic conditions. However, under constant light, this mutant showed a
578 reduced growth rate and was outcompeted by the wild-type cells in mixed cultures.
579 Photoheterotrophic and heterotrophic conditions were not tested in this study.
580 *Synechocystis* strains used in different laboratories can vary in their genome and
581 phenotypic characteristics, including glucose sensitivity (see for example[28, 72]). As the input
582 and output pathways of the new oscillator are unknown, it is possible that mutations in
583 different wild-type variants lead to variations in the expression of phenotypic effects in the
584 clock mutants.
585 Here, we demonstrate that KaiA3 is a novel KaiA homolog and element of the KaiC3-
586 based signaling pathway and has canonical KaiA functions. The N-terminal half of KaiA3
587 may still have a response regulatory function; however, the exact mechanism remains
588 unclear. Among other actions, KaiA3 must be placed within the regulatory and metabolic
589 networks of *Synechocystis*. Finally, our findings in the cyanobacterium *Synechocystis*
590 demonstrated the parallel presence of two circadian protein oscillators within a single cell.
591
592 **Materials and Methods**
593
594 *Reciprocal BLAST of Sll0485 (KaiA3) and Slr1783 (Rre1)*
595 Reciprocal BLAST was performed as described by Schmelling *et al*.[26]. The 2017 database
596 was used for comparison with existing data on other circadian clock proteins. The protein
597 sequences of Sll0485 (KaiA3) and Slr1783 (Rre1), as a reference for NarL response
598 regulators[43] from *Synechocystis,* were used as query sequences for this reciprocal
599 BLAST.
600
601 *Co-occurrence analysis*
602 The co-occurrence of KaiA3 with other circadian clock proteins in Cyanobacteria
603 containing KaiC1 was examined according to Schmelling *et al.*[26]. A right-sided Fisher's
604 exact test was used[73]. P-values were corrected for multiple testing after Benjamini-
605 Hochberg[74], with an excepted false discovery rate of 10^{-2}. All proteins were clustered
606 according to their corrected p-values.
607
608 *Synteny analyses using SyntTax*
609 The conservation of gene order was analyzed using the web tool 'SyntTax'[75];
610 https://pubmed.ncbi.nlm.nih.gov/23323735/. If not mentioned otherwise, default settings

611 (Best match, 10 % norm. BLAST) were applied. Chromosomes were selected manually
612 according to the results of Schmelling *et al*.[26].
613
614 *Multiple sequence alignments with Mafft and Jalview*
615 Sequence alignments, visualization, and analysis were performed with 'Jalview'[76]. The
616 sequences were aligned with Mafft, and if not mentioned otherwise, default settings (L-
617 INS-i, pairwise alignment computation method - localpair using Smith-Waterman
618 algorithm, gap opening penalty: 1.53, gap opening penalty at local pairwise alignment: -
619 2.00, group-to-group gap extension penalty: 0.123, matrix: BLOSUM62) were applied[77].
620 For analyses of the C-terminus, the alignments were trimmed to position 168 in the KaiA
621 reference sequence of *Synechococcus*. After trimming, the alignment was recalculated
622 with Mafft using the aforementioned default parameters.
623
624 *2D and 3D structure predictions*
625 The alignments generated in Jalview were then used with 'Ali2D' for secondary structure
626 prediction[78] [ref] https://toolkit.tuebingen.mpg.de). The identity cut-off to invoke a new
627 PSIPRED run was set to 30%. Three-dimensional protein structures were modeled using
628 either Phyre2 or SWISS-MODEL[79, 80]
629 (http://www.sbg.bio.ic.ac.uk/phyre2/html/page.cgi?id=index;
630 https://swissmodel.expasy.org/). The resulting structures were analyzed and illustrated
631 using UCSF Chimera[81] (https://www.cgl.ucsf.edu/chimera/).
632
633 *Phylogenetic reconstruction of protein trees*
634 Phylogenetic reconstruction of the protein trees of Sll0485 (KaiA3), Slr1783 (Rre1)/NarL
635 (*E. coli*, UniProtKB - P0AF28), and KaiA was achieved with MEGA X[82, 83] using the above
636 constructed alignments. For all alignments, a neighbor-joining tree and maximum
637 likelihood tree were constructed and compared. To construct neighbor-joining trees, 1000
638 bootstrap iterations with a p-distance substitution model and a gamma distribution with
639 three gamma parameters were used. To construct maximum likelihood trees, an initial tree
640 was constructed using the maximum parsimony algorithm. Further trees were constructed
641 using 1000 bootstrap iterations with an LG-G substitution model, a gamma distribution
642 with three gamma parameters, and nearest-neighbor-interchange (NNI) as the heuristic
643 method.
644
645 *Yeast two-hybrid assay*
646 AH109 yeast cells (Clontech) were used for yeast two-hybrid experiments. Transformation
647 of yeast cells was performed according to the manufacturer's guidelines using the Frozen-
648 EZ Yeast Transformation Kit (Zymo Research). Genes of interest were amplified from wild-
649 type genomic DNA using Phusion Polymerase (NEB), according to the manufacturer's
650 guidelines. The indicated restriction sites were introduced using oligonucleotides listed in
651 Table S1A. Vectors and PCR fragments were cut with the respective restriction enzymes,
652 and the gene of interest was ligated into the vector, leading to a fusion protein with a GAL4
653 activation domain (AD) or GAL4 DNA-binding domain (BD) either at the N- or C-terminus.

654 All constructed plasmids are listed in Table S2B. The detailed protocol for the growth
655 assay can be found in protocols.io (dx.doi.org/10.17504/protocols.io.wcnfave).
656 Successfully transformed cells were selected on a complete supplement mixture (CSM)
657 lacking leucine and tryptophan (-Leu -Trp) dropout medium (MP Biochemicals) at 30°C for
658 3-4 days. Cells containing bait and prey plasmids were streaked on CSM lacking leucine,
659 tryptophan, and histidine (-Leu -Trp -His) dropout medium (MP Biochemicals) with the
660 addition of 12.5 mM 3-amino-1,2,4-triazole (3-AT, Roth) and incubated for 6 days at 30°C
661 to screen for interactions.
662
663 *Expression and purification of recombinant Kai proteins*
664 *Synechocystis* KaiB3, KaiB1 and *Synechococcus* KaiA (plasmids kindly provided by T.
665 Kondo, Nagoya University, Japan) were produced as GST-fusion proteins in *E. coli*
666 BL21(DE3) as described in[25] (https://www.protocols.io/view/expression-and-purification-
667 of-gst-tagged-kai-prot-48ggztw). Briefly, proteins were purified by affinity chromatography
668 using glutathione-agarose 4 B (Macherey and Nagel), and the N-terminal GST-tag was
669 removed using PreScission Protease (Cytiva) prior to elution of the untagged proteins from
670 the glutathione resin. *Synechocystis* KaiC3 was produced with an N-terminal- Strep-tag
671 (Strep-KaiC3) in *E. coli* Rosetta-gami B (DE3) cells and purified via affinity
672 chromatography using Strep-tactin XT superflow (IBA-Lifesciences)[25]
673 (https://www.protocols.io/view/heterologous-expression-and-affinity-purification-
674 meac3ae). *The Synechocystis* ORF *sll0485,* encoding KaiA3, was inserted into the vector
675 pET22b to create a C-terminal His6-fusion. KaiA3-His6 was expressed in *E. coli* Tuner
676 (DE3) cells and purified by immobilized metal affinity chromatography (IMAC) using
677 PureProteome™ Nickel Magnetic Beads (Millipore). For a detailed protocol, see at
678 protocols.io (dx.doi.org/10.17504/protocols.io.bu5bny2n). Recombinant proteins were
679 stored at -80°C in buffer containing 20 mM Tris, pH 8.0, 150 mM NaCl, 0.5 mM EDTA, 5
680 mM $MgCl_2$, and 1 mM ATP.
681
682 *KaiC3 phosphorylation in* in vitro *assays and liquid chromatography mass spectrometry*
683 *(LC-MS/MS)*
684 Recombinant Strep-KaiC3 purified from *E. coli* exists mainly in its phosphorylated form
685 (KaiC3-P). Fully dephosphorylated Strep-KaiC3 (KaiC3-NP) was generated by incubating
686 the protein for 18 h at 30°C in assay buffer (20 mM Tris, pH 8.0, 150 mM NaCl, 0.5 mM
687 EDTA, 5 mM $MgCl_2$, and 1 mM ATP). The autokinase activity of KaiC3-NP was
688 investigated by incubating 0.2 µg/µl KaiC3 for 16 h at 30°C in 20 µl assay buffer in the
689 presence or absence of 0.1 µg/µl KaiA3-His6, KaiB3, and *Synechococcus* KaiA. Ten-
690 microliter aliquots were taken before and after incubation at 30°C, and the reaction was
691 stopped with SDS sample buffer. Samples were stored at -20°C prior to application to a
692 high resolution LowC SDS gel (10% T, 0.67% C)[84] using the Hoefer Mighty small II gel
693 electrophoresis system and Tris-Tricine running buffer (cathode buffer: 100 mM Tris, 100
694 mM Tricine, 0.1 % SDS, pH 8.25; anode buffer: 100 mM Tris, pH 8.9, according to
695 Schägger and von Jagow[85]). Gels were stained with Coomassie Blue R.

696 For the 48 h assay, pools containing 0.2 µg/µl (3.4 µM) KaiC3-NP, 0.1 µg/µl KaiB3 (7.4
697 µM) and various concentrations of KaiA3-His6 (corresponding to 0.5 – 8.4 µM) were
698 prepared in assay buffer supplemented with 5 mM ATP, split in 10 µl aliquots for the
699 desired timepoints and stored at -80°C. Samples were thawed on ice for 10 min prior to
700 incubation at 30°C for the different time periods. The reaction was stopped at specific time
701 points by adding SDS sample buffer. Samples were stored at -80°C prior to application to
702 a LowC SDS gel (10% T, 0.67% C)[26] sing the Biorad Mini PROTEAN gel electrophoresis
703 system and Tris-glycine running buffer (25 mM Tris, 192 mM glycine, 0.1 % SDS,
704 according to Laemmli[86]). The gels were stained with ROTI®Blue quick stain. In Tris-glycine
705 buffer, three KaiC3 bands could be separated, whereas two KaiC3 bands were separated
706 in Tris-Tricine buffer.
707 For LC-MS/MS- based analysis of KaiC3 phosphorylation sites, Strep-KaiC3 and KaiA3
708 were co-incubated *in vitro* as described above. Samples were taken directly after mixing,
709 as well as after 2 and 6 h of incubation, and separated by SDS-PAGE. For each sample,
710 protein-containing gel regions of Strep-KaiC size were cut out with a scalpel. For the 6 h
711 time point, a gel region at the potential size of the Strep-KaiC3/A3 complex was also
712 extracted. In-gel protein digestion with trypsin was performed as described by Shevchenko
713 *et al.* [87]. The generated peptides were extracted and purified using the stage tip protocol[88].
714 Of the resulting peptide solution, 20% was used for nanoLC-MS/MS analysis. Therefore,
715 peptides were separated in a 37 min reverse-phase linear gradient and directly ionized in
716 an online coupled ESI source upon elution for analysis on a Q Exactive HF mass
717 spectrometer (Thermo Fisher Scientific) operated in data-dependent acquisition mode.
718 The 12 highest abundant multiply charged ions of each full scan were separately
719 fragmented by HCD, and the generated fragment ions were analyzed in consecutive
720 MS/MS scans. Raw data files were processed using MaxQuant software (version 1.5.2.8)
721 and default settings. Phosphorylation of Ser, Thr, and Tyr was defined as a variable
722 modification. Acquired m/z spectra were searched against the proteome databases of
723 *Synechocystis* and *E. coli* (downloaded from cyanobase and Uniprot, respectively).
724 Annotated MS/MS spectra were visualized using the MaxQuant viewer.
725
726 *Clear native protein PAGE, Phos-tag SDS-PAGE and immunodetection*
727 Kai proteins (10 µl samples containing 2 µg dephosphorylated Strep-KaiC3, 1 µg KaiA3-
728 His6, 1 µg KaiB3, 1 µg *Synechococcus* KaiA) were incubated for 16 h at 30°C in
729 phosphorylation assay buffer, followed by separation of the native proteins in 4-16% native
730 PAGE at 4°C using a clear native buffer system (Serva) without anionic dye. Thus, only
731 proteins with a pI<7 at physiological pH were separated. Protein bands were visualized
732 with Coomassie staining (ROTIBlue Quick, Carl Roth) or immunodetected with a
733 monoclonal anti-His antibody conjugated to HRP (MA1-21315-HRP, Thermo Fisher,
734 1:2000 diluted). A detailed protocol can be found in protocols.io
735 (dx.doi.org/10.17504/protocols.io.bu67nzhn).
736 To analyze *the in vivo* phosphorylation of KaiC3, *Synechocystis* wild type, *ΔkaiA3,* and
737 *ΔkaiC3* cells were cultivated in BG11 or copper-depleted medium for *kaiA3*
738 overexpression. After an initial 12h/12h light/dark cycle, 10 ml of cells were collected every

739 6 h for analysis. The cells were cooled in liquid nitrogen for 5 s and harvested by
740 centrifugation (3220 × g, 2 min, 4°C). The pellet was frozen in liquid nitrogen and stored
741 at -20°C until further processing. To lyse the cells, the pellets were resuspended to an
742 OD_{750} of 25 in phosphorylation buffer (50 mM NaOH-HEPES pH 7.5, 300 mM NaCl, 0.5
743 mM Tris-(2-carboxyethyl)-phosphine, 10 mM $MgCl_2$). The cells were disrupted twice in a
744 cell mill at 30 Hz for 1 min at 4°C, using glass beads. The crude cell extract was obtained
745 by centrifugation (500 × g, 1 min, 4°C). For mobility shift detection of phosphorylated and
746 dephosphorylated KaiC3, a Zn^{2+}-Phos-tag® SDS-PAGE assay (Wako Chemicals) was
747 used. A 9% SDS-PAGE gel containing 25 µM Phos-tag acrylamide was prepared and 12
748 µL of cell extract was run at 150 V for 3 h at 4°C. Proteins were blotted onto a nitrocellulose
749 membrane (Amersham™ Protran®) via wet blotting. Immunodetection was performed
750 using αKaiC3[27] and anti-rabbit secondary (Thermo Fisher Scientific Inc., USA) antibodies.

751

752 *Screening of KaiC3 and KaiC1 binding partners by immunoprecipitation-coupled liquid*
753 *chromatography mass spectrometry (LC-MS/MS)*
754 *Synechocystis* WT/FLAG-*kaiC3*, WT/FLAG-*kaiC1*, and WT/FLAG-*sfGFP* (control) strains
755 were cultivated in BG11 medium (100 ml, copper-depleted) and harvested by
756 centrifugation at 6000 × *g* for 10 min at 4°C. According to Wiegard *et al.*[27], cells were
757 disrupted in a mixer mill, followed by solubilization with n-dodecyl-β-maltoside for 1 h. The
758 supernatant was used for FLAG purification in pull-down assays with Anti-Flag® M2
759 Magnetic Beads (Sigma-Aldrich), following the manufacturer's protocol. The resulting
760 elution fractions were loaded onto a NuPAGE™ Bis-Tris Gel and run following the
761 manufacturer's protocol (Invitrogen). Protein bands were allowed to migrate only a short
762 distance of approximately 10 mm. After staining the gel for 60 min with InstantBlue™
763 (Expedeon), the protein-containing gel regions were excised. Two independent replicates
764 were produced for each condition (KaiC3, KaiC1, or control pull-down). In-gel protein
765 digestion with trypsin was performed as described above, and the resulting peptide
766 solutions were purified using stage tips. Approximately 20% of the sample was applied for
767 nanoLC-MS/MS analysis as described above on a Q Exactive HF mass spectrometer
768 (Thermo Fisher Scientific) operated in the data-dependent acquisition mode. Raw data of
769 KaiC3 or KaiC1 pull-downs were separately processed using the MaxQuant software
770 (version 1.5.2.8) embedded MaxLFQ algorithm as described by Cox *et al.*[89]. Raw spectra
771 were searched against the proteome databases of *Synechocystis* and *E. coli* (downloaded
772 from cyanobase and Uniprot, respectively) and the bait protein sequences. Significantly
773 enriched proteins were identified by Perseus software (version 1.6.5.0) significance B
774 analysis with a p-value- of 0.01.
775
776 *Strains and growth conditions*
777 Wild-type *Synechocystis* (PCC-M, resequenced[28]), the deletion strains Δ*rpaA*[37], Δ*kaiC3*[25],
778 Δ*kaiA3*, and Δ*kaiA3B3C3* (Fig. S1), and complementation strain Δ*kaiA3*/*kaiA3* (Fig. S1)
779 were cultured photoautotrophically in BG11 medium[90] supplemented with 10 mM TES
780 buffer (pH 8) under constant illumination with 75 µmol photons m^{-2} s^{-1} of white light (Philips

781 TLD Super 80/840) at 30°C. Cells were grown either in Erlenmeyer flasks with constant
782 shaking (140 rpm) or on plates (0.75% Bacto-Agar; Difco) supplemented with
783 0.3% thiosulfate. For photomixotrophic experiments, 0.2% glucose was added to the
784 plates. For chemoheterotrophic growth experiments in complete darkness, *Synechocystis*
785 cells were spotted at different dilutions on BG11 agar plates containing 0.2% glucose and
786 incubated either mixotrophically for three days with continuous illumination or
787 chemoheterotrophically in the dark for 26 days.
788
789 *Construction of mutants of the KaiC3 based clock system*
790 To construct the *kaiA3* (*sll0485*) deletion strain, *Synechocystis* wild-type cells were
791 transformed with the plasmid pUC19-Δ*sll0485*. For plasmid construction, PCR products
792 were generated using the oligonucleotides P13-P14 and pUC19 as template, P15-P16
793 and P19-P20 with genomic *Synechocystis* wild-type DNA as template and P17-25 with
794 pUC4K as template. Homologous recombination led to replacement of the *sll0485* gene
795 with a kanamycin resistance cassette (Fig. S1). For genomic complementation of the
796 Δ*sll0485* strain, cells were transformed with the plasmid pUC19-Δ*sll0485*-compl.
797 Overlapping fragments were generated using the oligonucleotides P15-28 and P24-32
798 with genomic *Synechocystis* wild-type DNA as template, P13-P26 and pUC19 as
799 template, and P22-P23 and the vector pACYC184 as template. In the resulting
800 complementation strain Δ*kaiA3/kaiA3*, the kanamycin resistance cassette was replaced
801 with *sll0485*, and a chloramphenicol resistance cassette was introduced downstream of
802 the *kaiB3* gene (Fig. S1). For the triple-knockout mutant Δ*kaiA3B3C3,* Δ*kaiC3* cells were
803 used as the background strain for transformation with the pUC19-Δ*kaiA3B3* plasmid. PCR
804 products were generated using the oligonucleotides P13-P26 and pUC19 as template,
805 P17-P27 and pUC4K as template, P15-P16 and P25-P28 with genomic *Synechocystis*
806 wild-type DNA as template. The operon *kaiA3kaiB3* was replaced with a kanamycin
807 resistance cassette (Fig. S1). Complete segregation of the mutant alleles was confirmed
808 using PCR. For the Δ*kaiA3* strain, oligonucleotides P15-P29 were used. Segregation of
809 the complementation strain was confirmed by PCR with P15-P29, P30-P31, and P19-P32.
810 For the triple knockout mutant Δ*kaiA3B3C3,* deletion of the *kaiA3B3* operon was
811 confirmed by PCR using the primer pairs P15-P33 and P19-P30. The *kaiA3B3*
812 chromosomal region of the mutants is shown in Fig. S1.
813 Ectopic expression of *sll0485* was achieved in wild-type and Δ*sll0485* cells after
814 transformation with plasmid pUR-NFLAG-*sll0485*. The plasmid was constructed via
815 restriction digestion of the vector pUR-N-Flag-xyz, and the PCR product was amplified
816 with the oligonucleotide pair P29-P34 using genomic *Synechocystis* wild-type DNA as a
817 template. Restriction digestion with EcoRI and BamHI was followed by ligation. Successful
818 transformation was confirmed by PCR with P35-P36. The oligonucleotides and plasmids
819 used are listed in Table S1.
820
821 **Data availability**
822

The mass spectrometry proteomics data were deposited in the ProteomeXchange Consortium (http://proteomecentral.proteomexchange.org) via the PRIDE partner repository [91], with the dataset identifier PXD0042846.

Datasets S1 to S3 were deposited on a server and can be accessed under the following link:
https://supplements.biologie.uni-freiburg.de/the_non-standard_kaia3_regulator/
Information for reviewers: account: pilus, password: freecastle

Acknowledgments

We thank Research Unit FOR2816 'SCyCode' (The Autotrophy-Heterotrophy Switch in Cyanobacteria: Coherent Decision-Making at Multiple Regulatory Layers) funded by the German Research Foundation for fruitful discussions and financial support. This work was financially supported by grants (WI2014/5-3; 10-1; AX 84/1-3 and MA 4918/4-1) from the German Research Foundation to A.W., I.M.A., and B.M., respectively. We thank Pauline Morys, Annika Klopp, Isabell Bleile, Werner Bigott, and Petra Kolkhof for technical assistance.

843
844 **References**
845

846 1. Nakajima M*, et al.* Reconstitution of circadian oscillation of cyanobacterial KaiC
847 phosphorylation in vitro. *Science* **308**, 414-415 (2005).

848
849 2. Egli M, Mori T, Pattanayek R, Xu Y, Qin X, Johnson CH. Dephosphorylation of the Core
850 Clock Protein KaiC in the Cyanobacterial KaiABC Circadian Oscillator Proceeds via an ATP
851 Synthase Mechanism. *Biochemistry* **51**, 1547-1558 (2012).

852
853 3. Pattanayek R, Wang J, Mori T, Xu Y, Johnson CH, Egli M. Visualizing a Circadian Clock
854 Protein: Crystal Structure of KaiC and Functional Insights. *Molecular Cell* **15**, 375-388
855 (2004).

856
857 4. Terauchi K*, et al.* ATPase activity of KaiC determines the basic timing for circadian clock of
858 cyanobacteria. *Proc Natl Acad Sci U S A* **104**, 16377-16381 (2007).

859
860 5. Kim YI, Dong G, Carruthers CW, Golden SS, LiWang A. The day/night switch in KaiC, a
861 central oscillator component of the circadian clock of cyanobacteria. *Proc Natl Acad Sci U*
862 *S A* **105**, 12825-12830 (2008).

863
864 6. Iwasaki H, Nishiwaki T, Kitayama Y, Nakajima M, Kondo T. KaiA-stimulated KaiC
865 phosphorylation in circadian timing loops in cyanobacteria. *Proc Natl Acad Sci U S A* **99**,
866 15788-15793 (2002).

867
868 7. Pattanayek R, Egli M. Protein–Protein Interactions in the Cyanobacterial Circadian Clock:
869 Structure of KaiA Dimer in Complex with C-Terminal KaiC Peptides at 2.8 Å Resolution.
870 *Biochemistry* **54**, 4575-4578 (2015).

871
872 8. Chang Y-G, Kuo N-W, Tseng R, LiWang A. Flexibility of the C-terminal, or CII, ring of KaiC
873 governs the rhythm of the circadian clock of cyanobacteria. *Proc Natl Acad Sci U S A* **108**,
874 14431-14436 (2011).

875
876 9. Chang Y-G, Tseng R, Kuo N-W, LiWang A. Rhythmic ring-ring stacking drives the circadian
877 oscillator clockwise. *Proc Natl Acad Sci U S A* **109**, 16847-16851 (2012).

878
879 10. Nishiwaki T*, et al.* Role of KaiC phosphorylation in the circadian clock system of
880 *Synechococcus elongatus* PCC 7942. *Proc Natl Acad Sci U S A* **101**, 13927-13932 (2004).

881
882 11. Kitayama Y, Iwasaki H, Nishiwaki T, Kondo T. KaiB functions as an attenuator of KaiC
883 phosphorylation in the cyanobacterial circadian clock system. *The EMBO Journal* **22**, 2127-
884 2134 (2003).

885
886 12. Tseng R*, et al.* Cooperative KaiA–KaiB–KaiC Interactions Affect KaiB/SasA Competition in
887 the Circadian Clock of Cyanobacteria. *Journal of Molecular Biology* **426**, 389-402 (2014).

888
889 13. Rust MJ, Markson JS, Lane WS, Fisher DS, O'Shea EK. Ordered phosphorylation governs
890 oscillation of a three-protein circadian clock. *Science* **318**, 809-812 (2007).

891
892 14. Cohen SE, Golden SS. Circadian Rhythms in Cyanobacteria. *Microbiology and Molecular*
893 *Biology Reviews* **79**, 373-385 (2015).

894
895 15. Swan JA, Golden SS, LiWang A, Partch CL. Structure, function, and mechanism of the core
896 circadian clock in cyanobacteria. *Journal of Biological Chemistry* **293**, 5026-5034 (2018).

897
898 16. Snijder J, Axmann IM. The Kai-Protein Clock-Keeping Track of Cyanobacteria's Daily Life.
899 In: *Macromolecular Protein Complexes II: Structure and Function* (eds Harris JR, Marles-
900 Wright J) (2019).

901
902 17. Zhao C, Xu Y, Wang B, Johnson CH. *Synechocystis*: A model system for expanding the study
903 of cyanobacterial circadian rhythms. *Front Physiol* **13**, 1085959 (2022).

904
905 18. Schmelling NM, Scheurer N, Köbler C, Wilde A, Axmann IM. Diversity of Timing Systems in
906 Cyanobacteria and Beyond. In: *Circadian Rhythms in Bacteria and Microbiomes* (eds
907 Johnson CH, Rust MJ). Springer International Publishing (2021).

908
909 19. Loza-Correa M, Gomez-Valero L, Buchrieser C. Circadian clock proteins in prokaryotes:
910 Hidden rhythms? *Frontiers in Microbiology* **1**, 1-11 (2010).

911
912 20. Terrettaz C, Cabete B, Geiser J, Valentini M, Gonzalez D. KaiC-like proteins contribute to
913 stress resistance and biofilm formation in environmental Pseudomonas species. *Environ*
914 *Microbiol* **25**, 894-913 (2023).

915
916 21. Ma P, Mori T, Zhao C, Thiel T, Johnson CH. Evolution of KaiC-Dependent Timekeepers: A
917 Proto-circadian Timing Mechanism Confers Adaptive Fitness in the Purple Bacterium
918 *Rhodopseudomonas palustris*. *PLoS Genet* **12**, e1005922 (2016).

919
920 22. Pitsawong W*, et al.* From primordial clocks to circadian oscillators. *Nature* **616**, 183-189
921 (2023).

922
923 23. Kanesaki Y*, et al.* Identification of Substrain-Specific Mutations by Massively Parallel
924 Whole-Genome Resequencing of *Synechocystis* sp. PCC 6803. *DNA Research* **19**, 67-79
925 (2012).

926
927 24. Aoki S, Onai K. Circadian Clocks of *Synechocystis* sp. Strain PCC 6803,
928 *Thermosynechococcus elongatus*, *Prochlorococcus* spp., *Trichodesmium* spp. and Other
929 Species. In: *Bacterial Circadian Programs* (eds Ditty JL, Mackey SR, Johnson CH). Springer-
930 Verlag Berlin (2009).

931
932 25. Wiegard A*, et al. Synechocystis* KaiC3 displays temperature- And KaiB-dependent ATPase
933 activity and is important for growth in darkness. *J Bacteriol* **202**, 1-36 (2020).

934
935 26. Schmelling NM*, et al.* Minimal tool set for a prokaryotic circadian clock. *BMC Evolutionary*
936 *Biology* **17**, 169 (2017).

937
938 27. Wiegard A*, et al.* Biochemical analysis of three putative KaiC clock proteins from
939 *Synechocystis* sp. PCC 6803 suggests their functional divergence. *Microbiology* **159**, 948-
940 958 (2013).

941
942 28. Trautmann D, Voß B, Wilde A, Al-Babili S, Hess WR. Microevolution in cyanobacteria: Re-
943 sequencing a motile substrain of *Synechocystis* sp. PCC 6803. *DNA Research* **19**, 435-448
944 (2012).

945
946 29. Dörrich AK, Mitschke J, Siadat O, Wilde A. Deletion of the *Synechocystis* sp. PCC 6803
947 *kaiAB1C1* gene cluster causes impaired cell growth under light-dark conditions.
948 *Microbiology* **160**, 2538-2550 (2014).

949
950 30. Axmann IM*, et al.* Biochemical evidence for a timing mechanism in *Prochlorococcus*. *J*
951 *Bacteriol* **191**, 5342-5347 (2009).

952
953 31. Holtzendorff J, Partensky F, Mella D, Lennon JF, Hess WR, Garczarek L. Genome
954 streamlining results in loss of robustness of the circadian clock in the marine
955 cyanobacterium *Prochlorococcus marinus* PCC 9511. *J Biol Rhythms* **23**, 187-199 (2008).

956

957 32. Williams SB, Vakonakis I, Golden SS, LiWang AC. Structure and function from the circadian
958 clock protein KaiA of *Synechococcus elongatus*: a potential clock input mechanism. *Proc*
959 *Natl Acad Sci U S A* **99**, 15357-15362 (2002).

960
961 33. Vakonakis I, Sun J, Wu T, Holzenburg A, Golden SS, LiWang AC. NMR structure of the KaiC-
962 interacting C-terminal domain of KaiA, a circadian clock protein: implications for KaiA-KaiC
963 interaction. *Proc Natl Acad Sci U S A* **101**, 1479-1484 (2004).

964
965 34. Ye S, Vakonakis I, Ioerger TR, LiWang AC, Sacchettini JC. Crystal structure of circadian clock
966 protein KaiA from *Synechococcus elongatus*. *Journal of Biological Chemistry* **279**, 20511-
967 20518 (2004).

968
969 35. Kim YI, Vinyard DJ, Ananyev GM, Dismukes GC, Golden SS. Oxidized quinones signal onset
970 of darkness directly to the cyanobacterial circadian oscillator. *Proc Natl Acad Sci U S A*
971 **109**, 17765-17769 (2012).

972
973 36. Nishimura H*, et al.* Mutations in KaiA, a clock protein, extend the period of circadian
974 rhythm in the cyanobacterium *Synechococcus elongatu*s PCC 7942. *Microbiology* **148**,
975 2903-2909 (2002).

976
977 37. Köbler C, Schultz SJ, Kopp D, Voigt K, Wilde A. The role of the *Synechocystis* sp. PCC 6803
978 homolog of the circadian clock output regulator RpaA in day–night transitions. *Molecular*
979 *Microbiology* **110**, 847-861 (2018).

980
981 38. Sato SS, Shimoda Y, Muraki A, Kohara M, Nakamura Y, Tabata S. A large-scale protein
982 protein interaction analysis in *Synechocystis* sp. PCC 6803. *DNA Research* **14**, 207-216
983 (2007).

984
985 39. Baikalov I, Schröder I, Kaczor-Grzeskowiak M, Grzeskowiak K, Gunsalus RP, Dickerson RE.
986 Structure of the *Escherichia coli* response regulator NarL. *Biochemistry* **35**, 11053-11061
987 (1996).

988
989 40. Komarek J, Kaštovský J, Mares J, Johansen J. Taxonomic classification of cyanoprokaryotes
990 (cyanobacterial genera) 2014, using a polyphasic approach. *Preslia* **86**, 295-335 (2014).

991
992 41. Galperin MY. Structural classification of bacterial response regulators: Diversity of output
993 domains and domain combinations. *J Bacteriol* **188**, 4169-4182 (2006).

994

995 42. Dvornyk V, Mei Q. Evolution of *kaiA*, a key circadian gene of cyanobacteria. *Scientific*
996 *Reports* **11**, 9995 (2021).

997
998 43. Ashby MK, Houmard J. Cyanobacterial Two-Component Proteins: Structure,Diversity,
999 Distribution, and Evolution. *Microbiology and Molecular Biology Reviews* **70**, 472-509
1000 (2006).

1001
1002 44. Vakonakis I, LiWang AC. Structure of the C-terminal domain of the clock protein KaiA in
1003 complex with a KaiC-derived peptide: implications for KaiC regulation. *Proc Natl Acad Sci*
1004 *U S A* **101**, 10925-10930 (2004).

1005
1006 45. Delumeau O*, et al.* Functional and structural characterization of RsbU, a stress signaling
1007 protein phosphatase 2C. *Journal of Biological Chemistry* **279**, 40927-40937 (2004).

1008
1009 46. Iwasaki H, Taniguchi Y, Ishiura M, Kondo T. Physical interactions among circadian clock
1010 proteins KaiA, KaiB and KaiC in cyanobacteria. *The EMBO Journal* **18**, 1137-1145 (1999).

1011
1012 47. Clodong S*, et al.* Functioning and robustness of a bacterial circadian clock. *Molecular*
1013 *Systems Biology* **3**, 90 (2007).

1014
1015 48. Nakajima M, Ito H, Kondo T. In vitro regulation of circadian phosphorylation rhythm of
1016 cyanobacterial clock protein KaiC by KaiA and KaiB. *FEBS Letters* **584**, 898-902 (2010).

1017
1018 49. Lin J, Chew J, Chockanathan U, Rust MJ. Mixtures of opposing phosphorylations within
1019 hexamers precisely time feedback in the cyanobacterial circadian clock. *Proc Natl Acad*
1020 *Sci U S A* **111**, E3937-E3945 (2014).

1021
1022 50. Dvornyk V, Vinogradova O, Nevo E. Origin and evolution of circadian clock genes in
1023 prokaryotes. *Proc Natl Acad Sci U S A* **100**, 2495-2500 (2003).

1024
1025 51. Loza-Correa M*, et al.* The *Legionella pneumophila* kai operon is implicated in stress
1026 response and confers fitness in competitive environments. *Environ Microbiol* **16**, 359-381
1027 (2014).

1028
1029 52. Min H, Guo H, Xiong J. Rhythmic gene expression in a purple photosynthetic bacterium,
1030 Rhodobacter sphaeroides. *FEBS Letters* **579**, 808-812 (2005).

1031

1032 53. de Sousa Machado JN*, et al.* Autophosphorylation of the KaiC-like protein ArlH inhibits
1033 oligomerization and interaction with ArlI, the motor ATPase of the archaellum. *Molecular*
1034 *Microbiology* **116**, 943-956 (2021).

1035
1036 54. Dong P*, et al.* A dynamic interaction process between KaiA and KaiC is critical to the
1037 cyanobacterial circadian oscillator. *Scientific Reports* **6**, 25129 (2016).

1038
1039 55. Mori T*, et al.* Circadian clock protein KaiC forms ATP-dependent hexameric rings and binds
1040 DNA. *Proc Natl Acad Sci U S A* **99**, 17203-17208 (2002).

1041
1042 56. Yang X, Kang CM, Brody MS, Price CW. Opposing pairs of serine protein kinases and
1043 phosphatases transmit signals of environmental stress to activate a bacterial transcription
1044 factor. *Genes and Development* **10**, 2265-2275 (1996).

1045
1046 57. Eelderink-Chen Z, Bosman J, Sartor F, Dodd AN, Kovács ÁT, Merrow M. A circadian clock
1047 in a nonphotosynthetic prokaryote. *Science Advances* **7**, eabe2086 (2021).

1048
1049 58. Paulose JK, Wright JM, Patel AG, Cassone VM. Human Gut Bacteria Are Sensitive to
1050 Melatonin and Express Endogenous Circadian Rhythmicity. *PLoS One* **11**, e0146643
1051 (2016).

1052
1053 59. Schmitz O, Katayama M, Williams SB, Kondo T, Golden SS. CikA, a Bacteriophytochrome
1054 That Resets the Cyanobacterial Circadian Clock. *Science* **289**, 765-768 (2000).

1055
1056 60. Pattanayak Gopal K, Phong C, Rust Michael J. Rhythms in Energy Storage Control the
1057 Ability of the Cyanobacterial Circadian Clock to Reset. *Current Biology* **24**, 1934-1938
1058 (2014).

1059
1060 61. Ivleva NB, Gao T, Liwang AC, Golden SS. Quinone sensing by the circadian input kinase of
1061 the cyanobacterial circadian clock. *Proc Natl Acad Sci U S A* **103**, 17468-17473 (2006).

1062
1063 62. Kim P*, et al.* CikA, an Input Pathway Component, Senses the Oxidized Quinone Signal to
1064 Generate Phase Delays in the Cyanobacterial Circadian Clock. *J Biol Rhythms* **35**, 227-234
1065 (2020).

1066
1067 63. Pattanayak Gopal K, Lambert G, Bernat K, Rust Michael J. Controlling the Cyanobacterial
1068 Clock by Synthetically Rewiring Metabolism. *Cell Reports* **13**, 2362-2367 (2015).

1069

1070 64. Haydon MJ, Mielczarek O, Robertson FC, Hubbard KE, Webb AAR. Photosynthetic
1071 entrainment of the Arabidopsis thaliana circadian clock. *Nature* **502**, 689-692 (2013).

1072
1073 65. Anderson SL, McIntosh L. Light-activated heterotrophic growth of the cyanobacterium
1074 *Synechocystis* sp. strain PCC 6803: A blue-light-requiring process. *J Bacteriol* **173**, 2761-
1075 2767 (1991).

1076
1077 66. Narikawa R, Kohchi T, Ikeuchi M. Characterization of the photoactive GAF domain of the
1078 CikA homolog (SyCikA, Slr1969) of the cyanobacterium *Synechocystis* sp. PCC 6803.
1079 *Photochemical and Photobiological Sciences* **7**, 1253-1259 (2008).

1080
1081 67. Welkie DG*, et al.* Genome-wide fitness assessment during diurnal growth reveals an
1082 expanded role of the cyanobacterial circadian clock protein KaiA. *Proc Natl Acad Sci U S A*
1083 **115**, E7174-E7183 (2018).

1084
1085 68. Xu Y, Mori T, Johnson CH. Cyanobacterial circadian clockwork: roles of KaiA, KaiB and the
1086 kaiBC promoter in regulating KaiC. *The EMBO Journal* **22**, 2117-2126 (2003).

1087
1088 69. Xu Y*, et al.* Circadian Yin-Yang Regulation and Its Manipulation to Globally Reprogram
1089 Gene Expression. *Current Biology* **23**, 2365-2374 (2013).

1090
1091 70. Singh AK, Sherman LA. Pleiotropic effect of a histidine kinase on carbohydrate metabolism
1092 in *Synechocystis* sp. strain PCC 6803 and its requirement for heterotrophic growth. *J*
1093 *Bacteriol* **187**, 2368-2376 (2005).

1094
1095 71. Scheurer NM*, et al.* Homologs of Circadian Clock Proteins Impact the Metabolic Switch
1096 Between Light and Dark Growth in the Cyanobacterium *Synechocystis* sp. PCC 6803.
1097 *Frontiers in Plant Science* **12**, 675227 (2021).

1098
1099 72. Tichý M, Bečková M, Kopečná J, Noda J, Sobotka R, Komenda J. Strain of *Synechocystis*
1100 PCC 6803 with Aberrant Assembly of Photosystem II Contains Tandem Duplication of a
1101 Large Chromosomal Region. *Front Plant Sci* **7**, 648 (2016).

1102
1103 73. Fisher RA. On the Interpretation of χ^2 from Contingency Tables, and the Calculation of P.
1104 *Journal of the Royal Statistical Society* **85**, 87-94 (1922).

1105
1106 74. Benjamini Y, Hochberg Y. Controlling the False Discovery Rate: A Practical and Powerful
1107 Approach to Multiple Testing. *Journal of the Royal Statistical Society: Series B*
1108 *(Methodological)* **57**, 289-300 (1995).

1109
1110 75. Oberto J. SyntTax: A web server linking synteny to prokaryotic taxonomy. *BMC*
1111 *Bioinformatics* **14**, (2013).

1112
1113 76. Waterhouse AM, Procter JB, Martin DMA, Clamp M, Barton GJ. Jalview Version 2-A
1114 multiple sequence alignment editor and analysis workbench. *Bioinformatics* **25**, 1189-
1115 1191 (2009).

1116
1117 77. Katoh K, Standley DM. MAFFT multiple sequence alignment software version 7:
1118 Improvements in performance and usability. *Molecular Biology and Evolution* **30**, 772-780
1119 (2013).

1120
1121 78. Gabler F*, et al.* Protein Sequence Analysis Using the MPI Bioinformatics Toolkit. *Curr*
1122 *Protoc Bioinformatics* **72**, e108 (2020).

1123
1124 79. Kelley LA, Mezulis S, Yates CM, Wass MN, Sternberg MJE. The Phyre2 web portal for
1125 protein modeling, prediction and analysis. *Nature Protocols* **10**, 845-858 (2015).

1126
1127 80. Waterhouse A*, et al.* SWISS-MODEL: homology modelling of protein structures and
1128 complexes. *Nucleic Acids Research* **46**, (2018).

1129
1130 81. Pettersen EF*, et al.* UCSF Chimera - A visualization system for exploratory research and
1131 analysis. *Journal of Computational Chemistry* **25**, 1605-1612 (2004).

1132
1133 82. Kumar S, Stecher G, Li M, Knyaz C, Tamura K. MEGA X: Molecular evolutionary genetics
1134 analysis across computing platforms. *Molecular Biology and Evolution* **35**, 1547-1549
1135 (2018).

1136
1137 83. Stecher G, Tamura K, Kumar S. Molecular Evolutionary Genetics Analysis (MEGA) for
1138 macOS. *Molecular Biology and Evolution* **37**, 1237-1239 (2020).

1139
1140 84. Nishiwaki T*, et al.* A sequential program of dual phosphorylation of KaiC as a basis for
1141 circadian rhythm in cyanobacteria. *The EMBO Journal* **26**, 4029-4037 (2007).

1142
1143 85. Schägger H, von Jagow G. Tricine-sodium dodecyl sulfate-polyacrylamide gel
1144 electrophoresis for the separation of proteins in the range from 1 to 100 kDa. *Analytical*
1145 *Biochemistry* **166**, 368-379 (1987).

1146

1147 86. Laemmli UK. Cleavage of Structural Proteins during the Assembly of the Head of
1148 Bacteriophage T4. *Nature* **227**, 680-685 (1970).

1149
1150 87. Shevchenko A, Tomas H, Havliš J, Olsen JV, Mann M. In-gel digestion for mass
1151 spectrometric characterization of proteins and proteomes. *Nature Protocols* **1**, 2856-2860
1152 (2007).

1153
1154 88. Rappsilber J, Mann M, Ishihama Y. Protocol for micro-purification, enrichment, pre-
1155 fractionation and storage of peptides for proteomics using StageTips. *Nature Protocols* **2**,
1156 1896-1906 (2007).

1157
1158 89. Cox J, Hein MY, Luber CA, Paron I, Nagaraj N, Mann M. Accurate proteome-wide label-
1159 free quantification by delayed normalization and maximal peptide ratio extraction,
1160 termed MaxLFQ. *Molecular & Cellular Proteomics* **13**, 2513-2526 (2014).

1161
1162 90. Rippka R, Deruelles J, Herdman M, Waterbury JB, Stanier RY. Generic Assignments, Strain
1163 Histories and Properties of Pure Cultures of Cyanobacteria. *Microbiology* **111**, 1-61 (1979).

1164
1165 91. Perez-Riverol Y*, et al.* The PRIDE database and related tools and resources in 2019:
1166 improving support for quantification data. *Nucleic Acids Research* **47**, D442-D450 (2019).

1167

1168

Supplementary Information for

Two circadian oscillators in one cyanobacterium

Christin Köbler[a,1], Nicolas M. Schmelling[b,1], Alice Pawlowski[b,1], Philipp Spät[c], Nina M. Scheurer[a], Kim Sebastian[a], Lutz Berwanger[b], Boris Maček[c], Ilka M. Axmann[b], Anika Wiegard[b], Annegret Wilde[a,*]

[a]Institute of Biology III, Faculty of Biology, University of Freiburg, 79104 Freiburg, Germany; [b]Institute for Synthetic Microbiology, Biology Department, Heinrich Heine University Düsseldorf, 40225 Düsseldorf, Germany; [c]Department of Quantitative Proteomics, Interfaculty Institute for Cell Biology, Eberhard Karls University Tübingen, 72076 Tübingen, Germany

[1]C.K., N.M.S and A.P. contributed equally to this work.

*Prof. Dr. Annegret Wilde, Albert-Ludwigs-Universität Freiburg, Institut für Biologie III, Schänzlestr. 1, 79104 Freiburg, Germany, Phone: +49 (0) 761-20397828

Email: annegret.wilde@biologie.uni-freiburg.de

This PDF file includes:

Figures S1 to S10
Table S1

Other supplementary materials for this manuscript include the following:

Datasets S1 to S3 (online only under the following link):
https://supplements.biologie.uni-freiburg.de/the_non-standard_kaia3_regulator/
Information for reviewers: account: pilus, password: freecastle

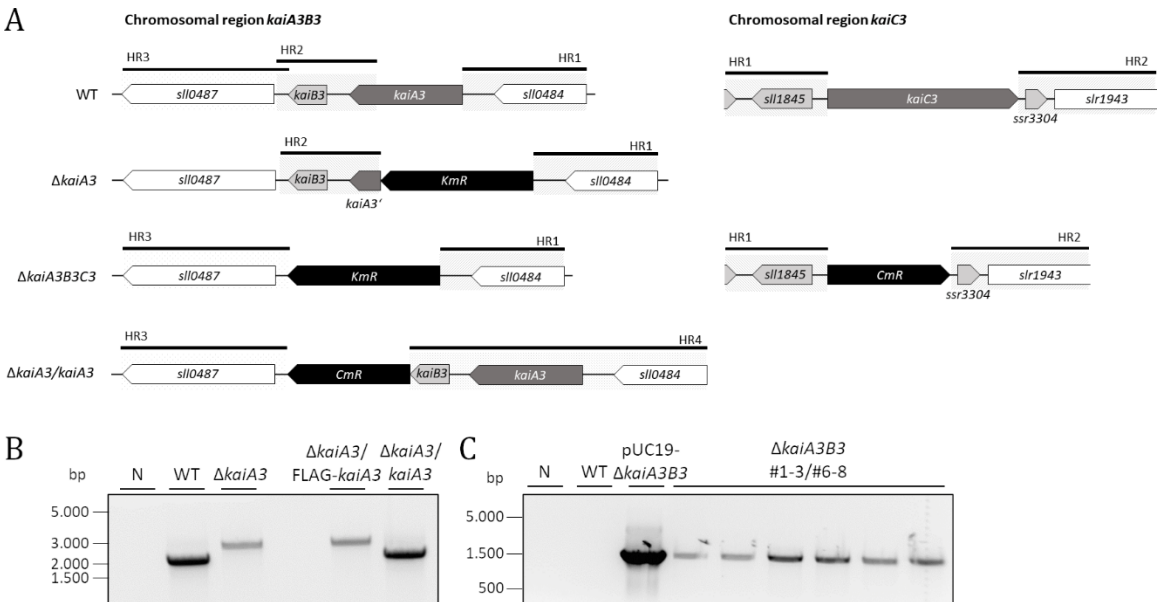

Fig. S1. Construction of mutants of the KaiC3 based clock system. (A) Schematic depiction of the *kaiA3B3 and* kaiC3 genomic context. Gene locus of *kaiA3B3* with the up- and downstream located genes. *KaiA3* and *kaiB3* are transcribed as an operon together with *sll0484*, the putative promotor is upstream of *sll0484*. For the inactivation of *kaiA3*, the gene was replaced by a kanamycin resistance cassette (KmR). For the construction of the triple knockout mutant Δ*kaiAB3C3*, the genomic region from *kaiA3* to *kaiB3* was replaced by a kanamycin resistance cassette (KmR) in the Δ*kaiC3* strain. Complementation of the Δ*kaiA3* strain was achieved by the introduction of *kaiA3* within its original genomic context with a chloramphenicol resistance cassette introduced downstream of the *kaiB3* gene. Clones were selected for chloramphenicol resistance and lack of kanamycin resistance. Black bars and grey, dashed boxes represent the regions for homologous recombination into the *Synechocystis* chromosome. (B) Representative result for the verification of the complete segregation of the Δ*kaiA3* deletion strain and Δ*kaiA3*/*kaiA3* complementation strain using colony PCR with the oligonucleotides P15-P29 (Table S1A). A non-template reaction (N), chromosomal WT DNA and Δ*kaiA3*/FLAG-*kaiA3* served as control reactions. Expected construct sizes are 1913 bp for the WT allele and Δ*kaiA3*/*kaiA3*, and 2472 bp for Δ*kaiA3* and Δ*kaiA3*/FLAG-*kaiA3*. (C) Verification of the *kaiA3B3* deletion in the Δ*kaiC3* strain using colony PCR with the oligonucleotides P15-P30. A non-template reaction (N), chromosomal WT DNA and the vector pUC19-Δ*kaiA3B3* served as control reactions. Expected construct size for Δ*kaiA3B3* and pUC19-Δ*kaiA3B3* is 1554 bp. No construct was expected for the WT allele. Complete segregation was verified with the oligonucleotides P19-P30 (not shown).

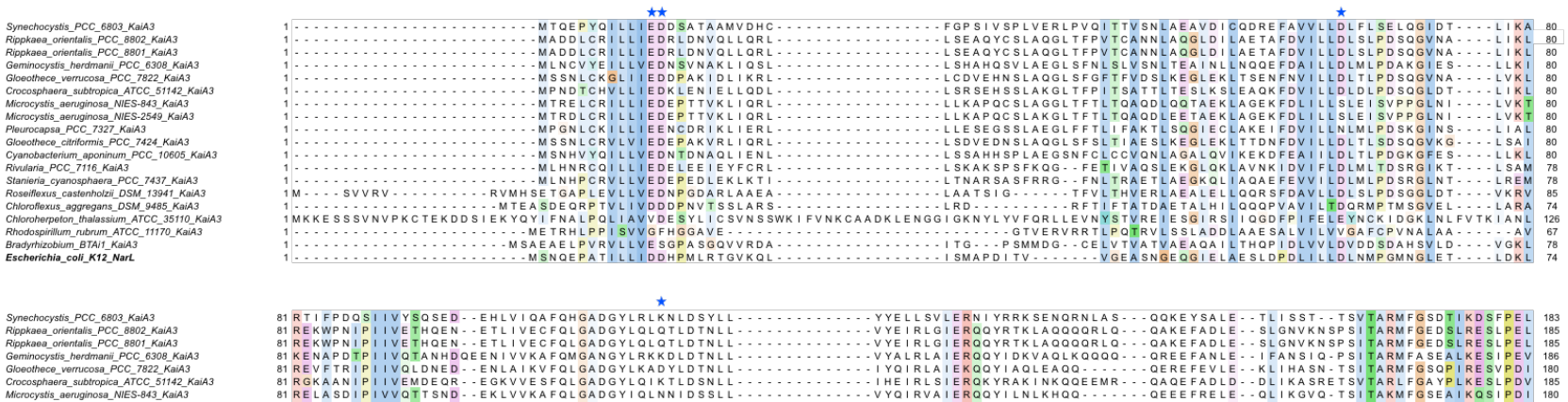

Fig. S2. Alignment of the amino acid sequences of Sll0485 (KaiA3) orthologs including NarL from *E. coli*. The sequences were aligned with Mafft (preset, L-INS-i). (A) Sequences are represented in the Clustalx color code with conservation visibility set 20 %[1, 2, 3]. As a representative of NarL-type response regulators, the NarL homolog of the *E. coli* strain K12 (UniProtKB - P0AF28) was added. The residues crucial for phosphorylation in response regulators are marked with a blue star[4].

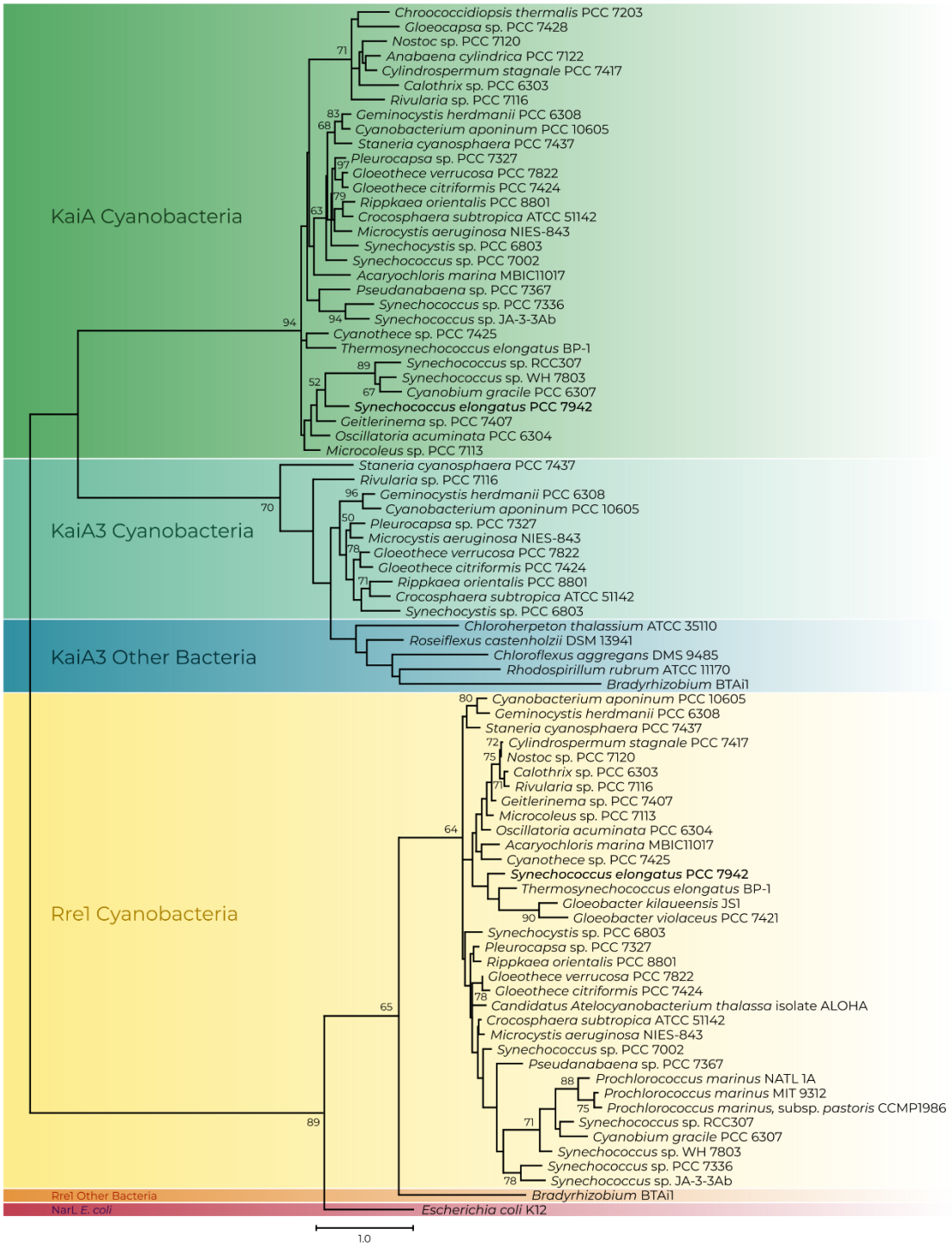

Fig. S3. Maximum likelihood-inferred phylogenetic reconstruction of selected orthologs of Sll0485 (KaiA3), Slr1783 (Rre1) and KaiA as well as NarL from *E. coli* (UniProtKB - P0AF28). The sequences were aligned with Mafft (L-INS-i default parameters, Jalview), trimmed to position 168 of the C-terminus of the *Synechococcus elongatus* PCC 7942 KaiA. Aligned sequences were used to infer an unrooted maximum likelihood protein tree. The scale bar indicates 1 substitution per position. Bootstrap values (n=1000) are displayed at branches. Bootstrap values less than 50 are not shown.

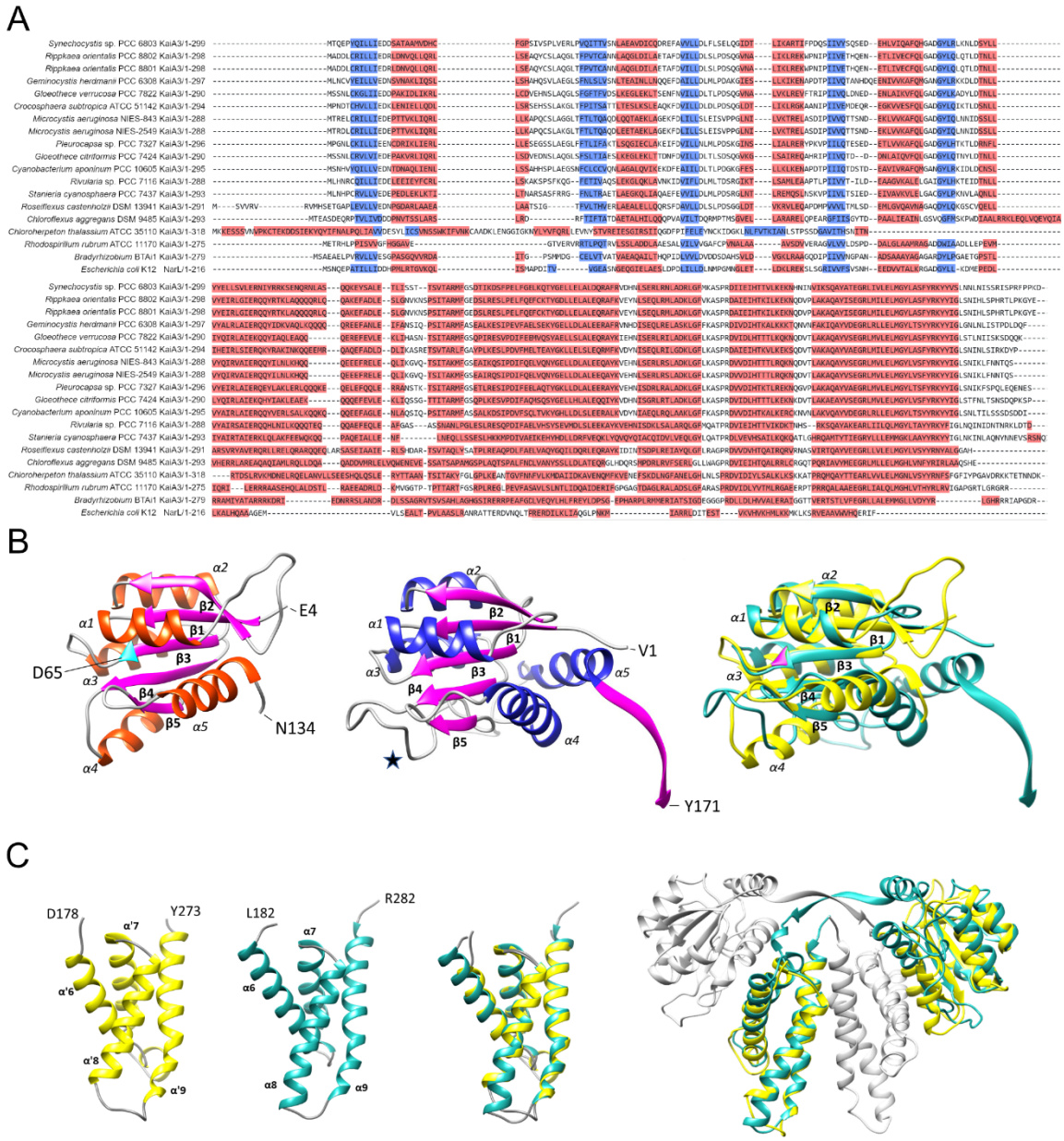

Fig. S4. Secondary structure prediction and modelling of KaiA3. (A) Sequence alignment (Fig. S2) was followed by a secondary structure prediction with Ali2D (preset, 30 % identity cutoff to invoke a new PSIPRED run). Predicted α-helices and β-strands are shown in red and blue, respectively[5]; https://toolkit.tuebingen.mpg.de. (B) The structure of the N-terminal domain of KaiA3 is closely similar to the PsR domain of KaiA. Left: The 3-D structure of the KaiA3 N-terminal domain (template *E. coli* NarL, PDB 1A04) was modelled with SWISS-Model (https://swissmodel.expasy.org/). It comprises residues E4-N134 (initial search with residues 1-140) and displays the canonical fold of a response regulator domain: a five-stranded α/β fold with a central five-stranded parallel β-sheet flanked on both faces by five amphipathic α-helices. The predicted phosphorylation site D65 is shown in turquoise. Middle: The PsR domain of *Synechococcus elongatus* PCC 7942 KaiA (template PDB 4G86, residues 1-171 shown) lacks the α4-helix (highlighted by an asterisk) as well as a phosphorylation site. Right: The predicted structure of the KaiA3 N-terminus (shown in yellow) superimposes well on the PsR domain of KaiA (shown in light sea green). The putative phosphorylatable aspartate in the KaiA3 β3-sheet is shown in pink. (C) The structure of the C-terminal domain of KaiA3 displays a KaiA-like motif. Left (yellow): The 3-D structure of the KaiA3

C-terminal domain (template KaiA *Thermosynechococcus elongatus* PDB 1V2Z) was modelled with SWISS-Model (https://swissmodel.expasy.org/). It comprises residues D178 – Y273 (initial search with residues 141- 299) and displays a KaiA-like four helix bundle (α'6 - α'9). Left (light sea green): The C-terminal domain of *Synechococcus elongatus* PCC 7942 KaiA (template PDB 4G86, residues 182 - 282). Numbering of the helices according to Ye *et al*.[4]. Middle: Superimposition of the KaiA3 C-terminal domain model structure on the KaiA C-terminus. Right: Superimposition of both KaiA3 domains on the chain B of the KaiA dimer (PDB 4G86). KaiA3 structures are shown in yellow, KaiA structures in light sea green.

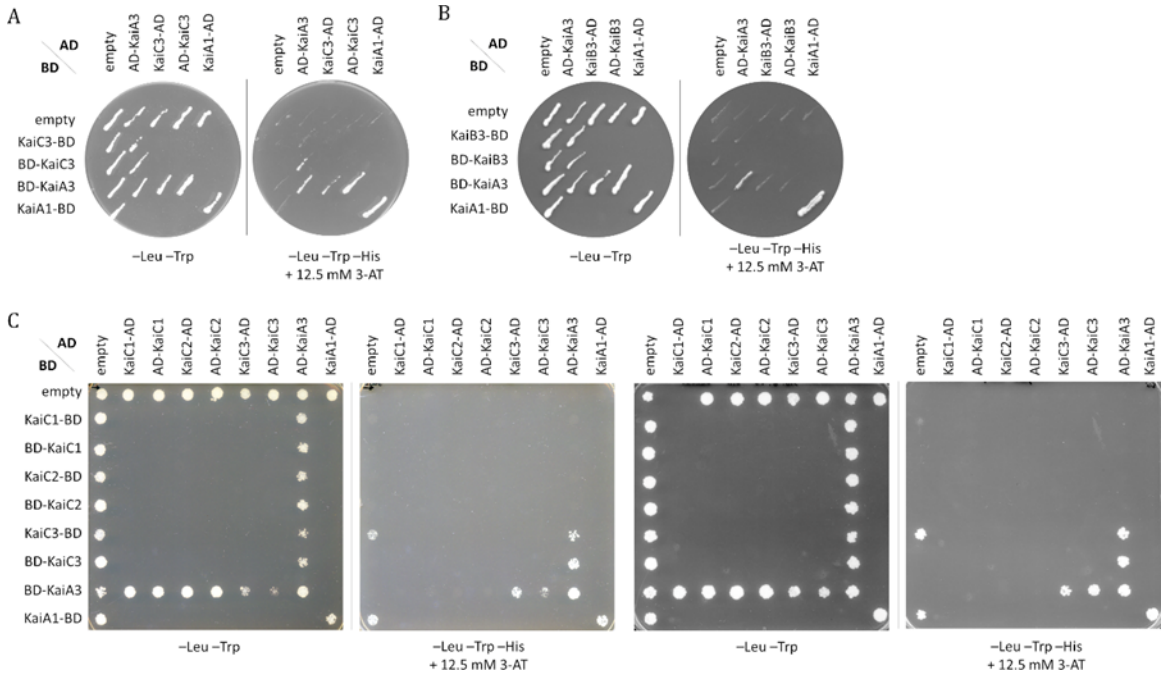

Fig. S5. Complete scans of the plates for KaiA3 interaction analysis with KaiB3 and the three KaiC homologs (KaiC1-KaiC3). Yeast two-hybrid reporter strains carrying the respective bait and prey plasmids, were selected by plating on complete supplement medium (CSM) lacking leucine and tryptophan (-Leu -Trp). As a positive control, *Synechocystis* KaiA dimer interaction was used. AD, GAL4 activation domain; BD, GAL4 DNA-binding domain. (A-C) Physical interaction between bait and prey fusion proteins is determined by growth on complete medium lacking leucine, tryptophan and histidine (-Leu -Trp -His) and addition of 12.5 mM 3-amino-1,2,4-triazole 88 (3-AT).

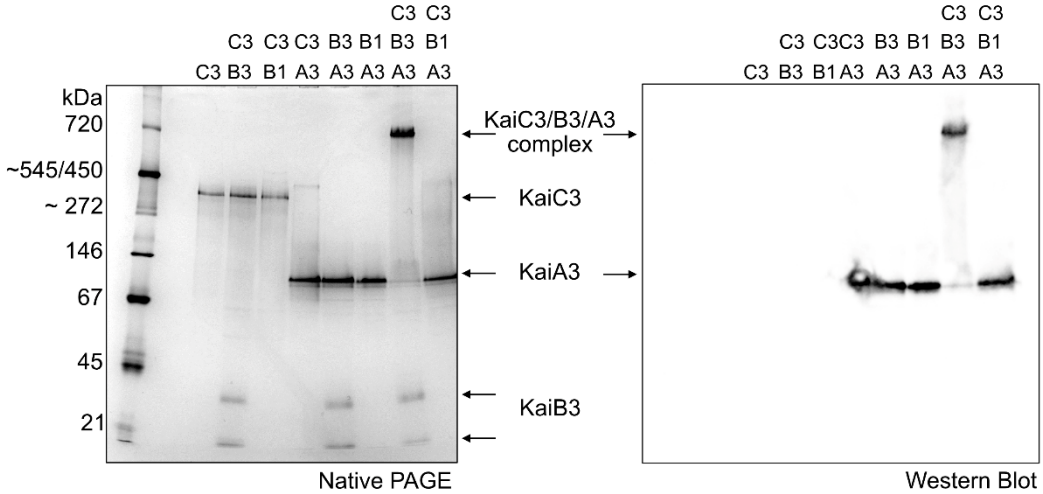

Fig. S6. KaiB1 does not form a complex with KaiA3 and KaiC3. Proteins were incubated for 16 h at 30 °C and subsequently subjected to 4-16% clear native PAGE. Gels were either stained with Coomassie Blue (left) or blotted and immunodecorated with a monoclonal anti-His antibody for the detection of recombinant KaiA3-His6 (right). Arrows indicate monomers or protein complexes. The KaiB1 monomer (12 kDa) is not visible in the 4-16% native gradient gel. In contrast to Fig. 2B, a faint band appears in the KaiA3/KaiC3 sample, which is shifted in comparison to the other KaiC3 bands (left). However, KaiA3 is not immunodetected in the shifted band (right).

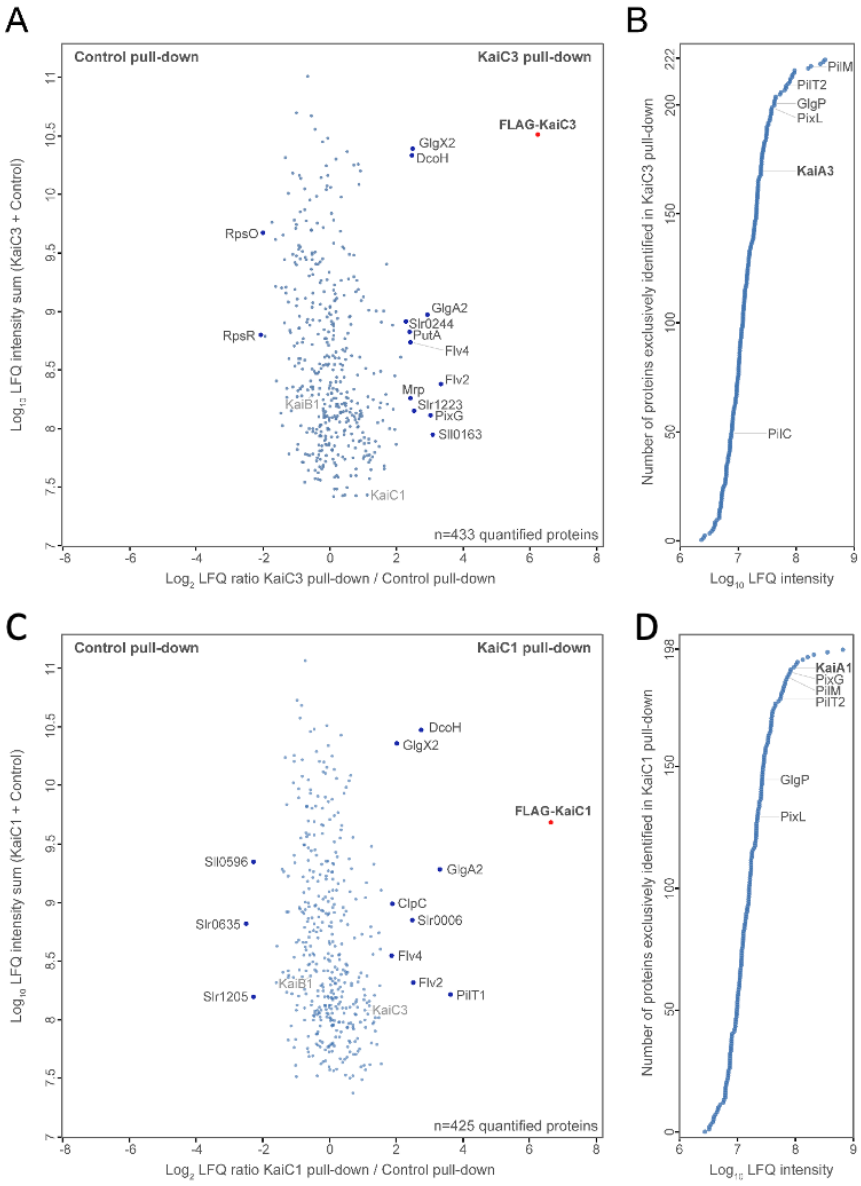

Fig. S7. Immunoprecipitation-coupled LC-MS/MS screening of KaiC3 (A, B) and KaiC1 (C, D) binding partners. Solubilized cell lysate of WT/FLAG-*kaiC3* (A), WT/FLAG-*kaiC1* (C) and WT/FLAG-*sfGFP* (control) strains were cultured under continuous light conditions in copper-depleted BG11 medium and used for α-FLAG co-immunoprecipitation in pull-down assays. After FLAG-purification, the elution fractions were analyzed by LC-MS/MS. Label-free quantification using the MaxQuant MaxLFQ algorithm was applied to identify co-enriched proteins. Panels A, C include quantified proteins which were detected in the FLAG-KaiC3 or FLAF-KaiC1 overexpression strain and the control strain. Log_2 LFQ ratios of FLAG-KaiC / control are plotted against the log_{10} LFQ intensity. Significantly enriched proteins (p-value = 0.01), labeled in dark grey font, are potential interaction partners of KaiC3 or KaiC1. (B, D) Panels include proteins which were exclusively identified in the FLAG-KaiC3 (B) or KaiC1 (D) pull-down, but not in the control. Proteins were sorted by their abundance in the KaiC co-immunoprecipitation eluates and selected proteins were labeled. A full list of identified proteins is shown in Data S2.

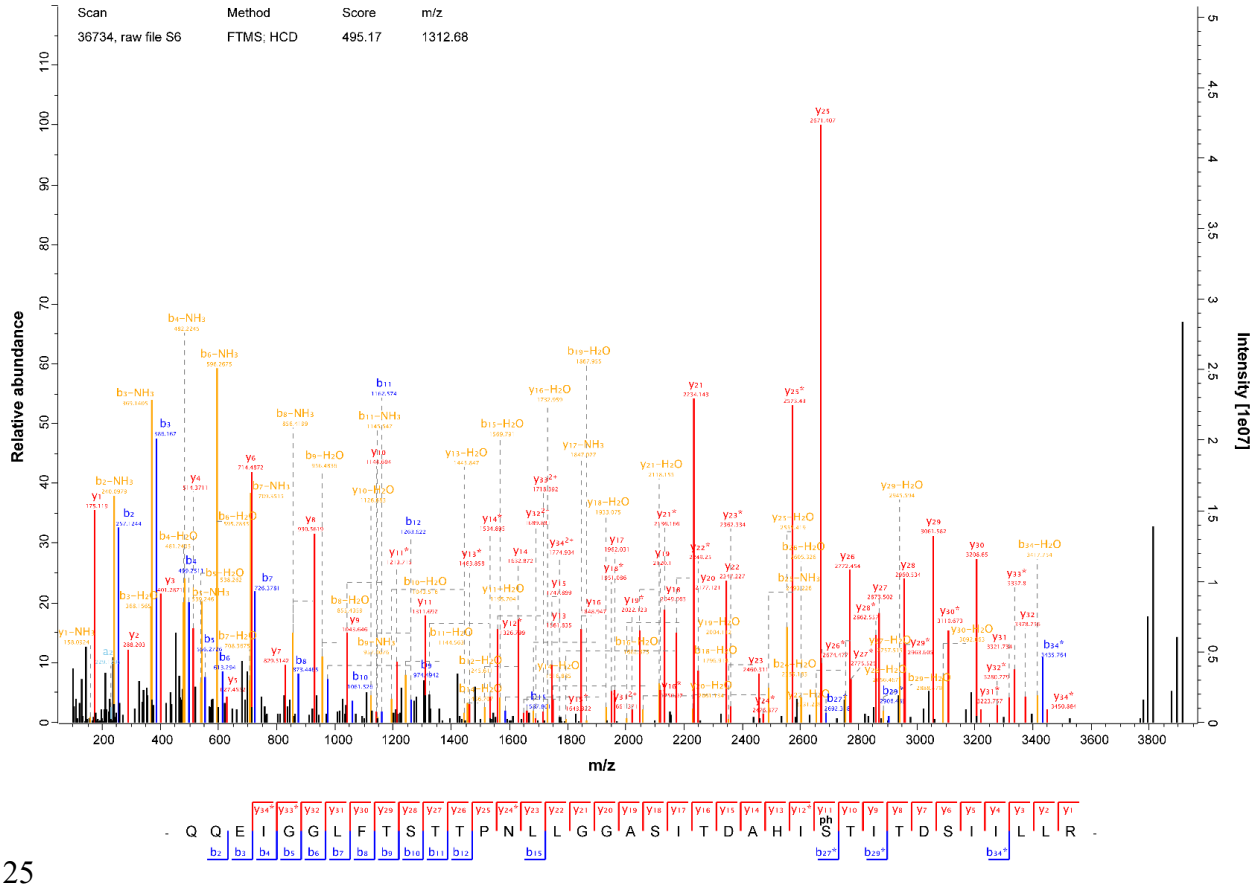

Fig. S8. Representative phosphopeptide of KaiC3 detected by mass spectrometry. Samples from KaiC3-KaiA3 *in vitro* co-incubation assays (see materials and method KaiC3 phosphorylation in in vitro assays and liquid chromatography mass spectrometry (LC-MS/MS))were digested with trypsin and analyzed by LC-MS/MS analysis. Comprehensive b- and y-ion series of an abundant, singly phosphorylated 37 amino acid peptide could be detected, localizing the phosphorylation site on Ser423 (position 27 in the peptide). In multiple cases, phosphorylation could be localized on the neighboring Thr424 position instead. Both sites are homologous positions to the KaiC1 auto-phosphorylation sites Ser432 and Thr433 and appeared with increased abundance after prolonged KaiC3-KaiA3 co-incubation duration.

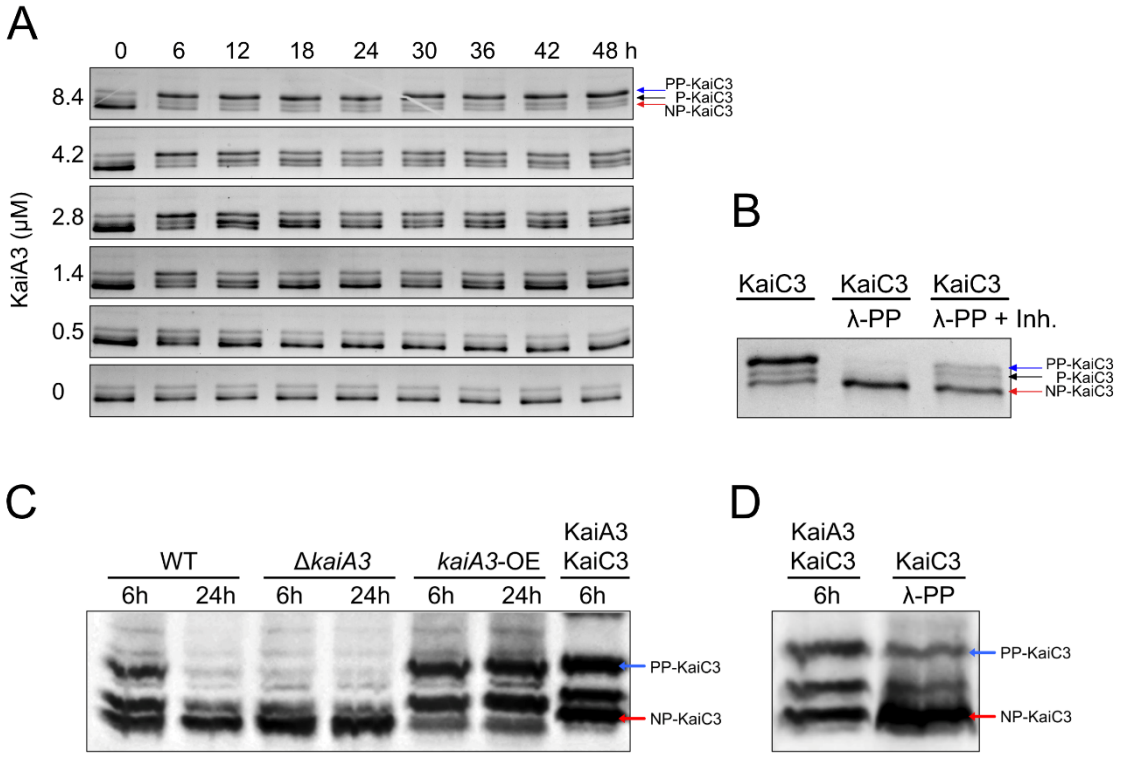

Fig. S9: In vitro and in vivo phosphorylation of KaiC3 in dependence of KaiA3. (A) In vitro phosphorylation of KaiC3 in the presence of 7.4 μM KaiB3 and varying concentrations of KaiA3. Representative gel images from 1 assay used for quantification of PP-KaiC3/total KaiC3 displayed in Fig. 3A. (B) KaiC3 was dephosphorylated by incubation with Lambda phosphatase (KaiC3/λ-PP) for 18h at 30°C and separated via high-resolution LowC SDS-PAGE as in A. As control, Lambda-phosphatase activity was blocked by addition of PhosSTOP (Roche) and 10 mM vanadate (KaiC3/λ-PP +Inh.). (C) Comparison of in vivo and in vitro phosphorylation of KaiC3. Whole cell extracts of *Synechocystis* wild-type (WT), *kaiA3* mutant (*ΔkaiA3*), and the overexpression (*kaiA3*-OE) strain, grown in a 12-h light/dark cycle, were subjected to Phos-tag SDS-PAGE followed by western blot analysis with a KaiC3-specific antibody. According to the data shown in Fig. 3C, KaiC3 is in a highly phosphorylated state at 6 h and mostly dephosphorylated at 24 h. For comparison, purified and in vitro phosphorylated KaiC3 were applied to the same gel. (D) KaiC3 was dephosphorylated (KaiC3/PP) using Lambda phosphatase (NEB), applied to a Phos-tag SDS-PAGE and Western blot analysis alongside with in vitro phosphorylated KaiC3, confirming that the fast migrating band of KaiC3 represents the dephosphorylated form of KaiC3. KaiC3 was phosphorylated in vitro in a mixture with KaiA3 (4.2 μM) for 6 h at 30°C (KaiA3-KaiC3/6h).

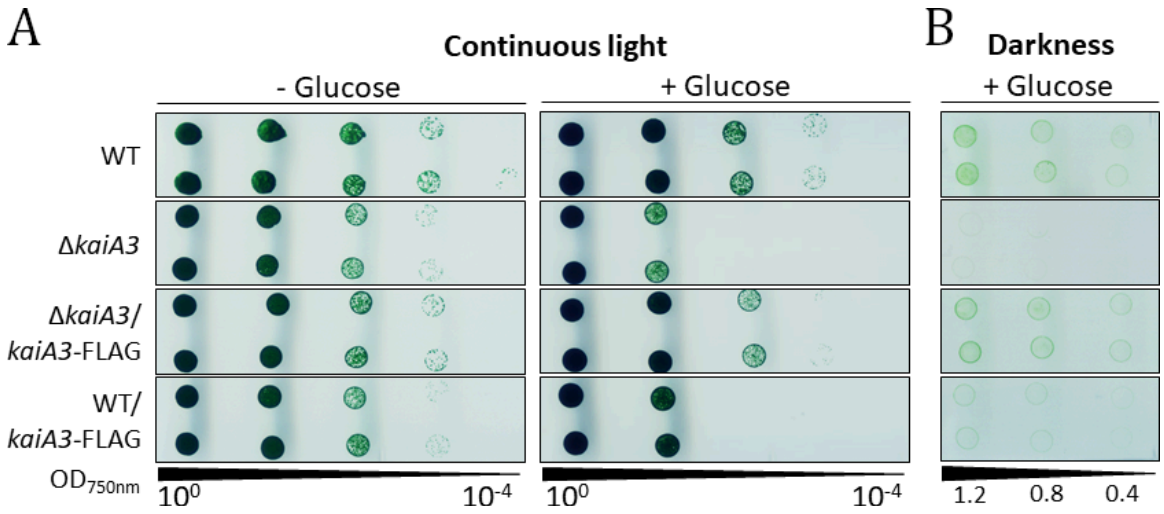

Fig. S10. Overaccumulation of *kaiA3* results in growth defects during mixotrophic and chemoheterotrophic growth. Proliferation of the WT, the *kaiA3* deletion mutant, and the strains Δ*kaiA3*/*kaiA3*-FLAG *and* WT/*kaiA3*-FLAG, expressing *kaiA3* ectopically from a self-replicating plasmid, was tested under phototrophic (continuous light, - glucose), photomixotrophic (continuous light, + glucose) and heterotrophic (darkness, + glucose) conditions. Strains were grown in liquid culture under constant light, different dilutions were spotted on agar plates and incubated in the indicated conditions with 75 µmol photons m^{-2} s^{-1} white light (A) or in darkness (B). A representative result of three independent experiments is shown. (A) Cultures were diluted to OD_{750nm} value 0.4 and dilution series were spotted on agar plates with or without the addition of 0.2% glucose. Plates were analyzed after 6 days of continuous light. (B) Cultures were diluted to OD_{750nm} values of 1.2, 0.8 and 0.4 and spotted on agar plates supplemented with 0.2% glucose. Plates were analyzed after 26 days of darkness. For expression of the *kaiA3*-FLAG gene from the P_{petJ} promoter in the overexpressor strains, all experiments were performed in medium lacking copper.

170 **Table S1.**

171 **A. Oligonucleotides used in this study.** Restriction sites are underlined. Overlaps used for
172 aqua cloning are marked in bold.

Primer	Oligonucleotide Name	Sequence (5‘ – 3‘)	Purpose[#]
	Construction of yeast two-hybrid expression vectors		
P1	BD-Sll0485-fw	TTGGATCCTACCCAGGAGCCCTACCAAATTC	Y2H
P2	BD-Sll0485-rev	GCACTAGTAGAACTATCTTTGGGGGGAAATCG	Y2H
P3	Sll0485-AD-fw	TAGGATCCATGACCCAGGAGCCCTACCA	Y2H
P4	Sll0485-AD-rev	GCCGCTCTAGAAGAACTATCTTTGGGGGGAAATC	Y2H
P5	KaiC2-AD-fw	TAGGATCCATGACAGATAACAGCCAAAG	Y2H
P6	KaiC2-AD-rev	GACCTAGGGGGGTTTTGATAAATGTG	Y2H
P7	AD-KaiC2-fw	TAGGATCCATACAGATAACAGCCAAAGTCTC	Y2H
P8	AD-KaiC2-rev	GACTCGAGGGGGTTTTGATAAATGTG	Y2H
P9	BD-KaiC2-fw	TAGGATCCAACAGATAACAGCCAAAGTCTC	Y2H
P10	BD-KaiC2-rev	TACCTAGGGGGGTTTTGATAAATGTG	Y2H
	Construction of *E. coli* expression vectors		
P11	1297_*sll0485*_Nde_fw	AATACATATGACCCAGGAGCCCTA	E
P12	1298_*sll0485*_Xho_rev	TATTCTCGAGAGAACTATCTTTGGGG	E
	Construction of vectors used for deletion and complementation mutants		
P13	pUC19-*sll0485*-fw	GCATTGCCATGGGCAA**GAATTCACTGGCCGTC**	MU
P14	pUC19-*sll0485*-rev	CCCATTCCTCTGGCG**GCAAGCTTGGCGTAATC**	MU
P15	US-*sll0485*-fw	**GACGGCCAGTGAATTC**TTGCCCATGGCAATGC	MU, CP
P16	US-*sll0485*-rev	**GACACAACGTGGCTTTCC**GTAATCACGGCTAAGTTC	MU
P17	*sll0485*-KmR-fw	**CTTAGCCGTGATTAC**GGAAAGCCACGTTGTGTC	MU
P18	*sll0485*-KmR-rev	**AACCTAGGCGATCGGC**GAGGTCTGCCTCGTGAAG	MU
P19	DS-*sll0485*-fw	**TCACGAGGCAGACCTC**GCCGATCGCCTAGGTT	MU, CP
P20	DS-*sll0485*-rev	**GATTACGCCAAGCTTGC**CGCCAGAGGAATGGG	MU, CP
P21	US-*sll0485*-compl-rev	**GTATCAACAGGGACAC**TTAATCCTCCGGCAAACG	MU
P22	CmR-*sll0485*-compl-fw	**TTTGCCGGAGGATTAA**GTGTCCCTGTTGATAC	MU
P23	CmR-*sll0485*-compl-rev	**GCCTAGGGGATAGCGG**CCAGCAATAGACATAAGC	MU
P24	DS-*sll0485*-compl-fw	**TTATGTCTATTGCTGG**CCGCTATCCCCTAGG	MU
P25	DS-*sll0485*-compl-rev	**GATTACGCCAAGC**TTGCCTATGAGTTGCCGAGG	MU
P26	pUC19-*sll0485*-compl-rev	**CCTCGGCAACTCATAG**GCAAGCTTGGCGTAATC	MU
P27	*kaiA3B3*-KmR-rev	**GCCTAGGGGATAGCGG**GAGGTCTGCCTCGTGAAG	MU
P28	DS-*kaiA3B3*-fw	**TCACGAGGCAGACCTC**CCGCTATCCCCTAGG	MU
P29	NFLAG-*sll0485*-rev	GGATCCTTAAGAACTATCTTTGGGG	MU, CP
P30	*kaiB3*-AD-rev	GCTCTAGAATCCTCCGGCAAACG	CP
P31	Km-seq-rev	GTATTTCGTCTCGCTCAGGC	CP
P32	Cm-seq-leftout	GCTCCTGAAAATCTCGATAACTC	CP
P33	Km-seg-fw	GCCTGAGCGAGACGAAATAC	CP
P34	NFLAG-*sll0485*-fw	GAATTCACCCAGGAGCCCTAC	MU
P35	pSK9-ORF-fw	CTCCCATAATACCTTCGCGTC	CP
P36	pUR-rev	CTTCCAGATGTATGCTCTTCTGCTC	CP

173
174 [#] CP, colony PCR; E, expression; MU, mutagenesis; Y2H, expression in yeast cells.
175
176

177 **B. Plasmids used in this study.**

Plasmid Name	Description	Reference
pCGADT7ah	Expression of fusion proteins with a C-terminal GAL4$_{(768–881)}$ AD-tag in yeast cells, LEU2, HA epitope tag	Rausenberger *et al.*,[6]
pGADT7ah	Expression of fusion proteins with an N-terminal GAL4$_{(768–881)}$ AD-tag in yeast cells, LEU2, HA epitope tag	Hiltbrunner *et al.,*[7]
pD153	Expression of fusion proteins with a C-terminal GAL4$_{(1–147)}$ DNA-BD-tag in yeast cells, TRP1, c-Myc epitope tag	Shimizu-Sato *et al.*,[8]
pGBKT7	Expression of fusion proteins with an N-terminal GAL4$_{(1–147)}$ DNA-BD-tag in yeast cells, TRP1, c-Myc epitope tag	Clontech, Germany
pGBK-BD-*sll0485*	Expression of Sll0485 with an N-terminal GAL4(1–147) DNA-BD-tag in yeast cells, *TRP1*, c-Myc epitope tag	This study
pGAD-AD-*sll0485*	Expression of Sll0485 with an N-terminal *GAL4*(768–881) AD-tag in yeast cells, *LEU2*, HA epitope tag	This study
pCGAD-*kaiC3*-AD	Expression of KaiC3 with a C-terminal *GAL4*(768–881) AD-tag in yeast cells, *LEU2*, HA epitope tag	Wiegard *et al.,*[9]
pGAD-AD-*kaiC3*	Expression of KaiC3 with an N-terminal GAL4$_{(768–881)}$ AD-tag in yeast cells, LEU2, HA epitope tag	Wiegard *et al.,*[9]
pD153-*kaiC3*-BD	Expression of KaiC3 with a C-terminal GAL4(1–147) DNA-BD-tag in yeast cells, *TRP1*, c-Myc epitope tag	Köbler *et al.*,[10]
pGBKT7-BD-*kaiC3*	Expression of KaiC3 with an N-terminal GAL4(1–147) DNA-BD-tag in yeast cells, *TRP1*, c-Myc epitope tag	Wiegard *et al.,*[9]
pCGAD-*kaiB3*-AD	Expression of KaiB3 with a C-terminal *GAL4*(768–881) AD-tag in yeast cells, *LEU2*, HA epitope tag	Wiegard *et al.,*[9]
pGAD-AD-*kaiB3*	Expression of KaiB3 with an N-terminal *GAL4*(768–881) AD-tag in yeast cells, *LEU2*, HA epitope tag	Wiegard *et al.,*[9]
pCGAD-*kaiA*-AD	Expression of KaiA with a C-terminal *GAL4*(768–881) AD-tag in yeast cells, *LEU2*, HA epitope tag	Köbler *et al.*,[10]
pD153-*kaiA*-BD	Expression of KaiA with a C-terminal GAL4(1–147) DNA-BD-tag in yeast cells, *TRP1*, c-Myc epitope tag	Köbler *et al.*,[10]
pCGAD-*kaiC1*-AD	Expression of KaiC1 with a C-terminal *GAL4*(768–881) AD-tag in yeast cells, *LEU2*, HA epitope tag	Köbler *et al.*,[10]
pGAD-AD-*kaiC1*	Expression of KaiC1 with an N-terminal *GAL4*(768–881) AD-tag in yeast cells, *LEU2*, HA epitope tag	Köbler *et al.*,[10]
pD153-*kaiC1*-BD	Expression of KaiC1 with a C-terminal GAL4$_{(1–147)}$ DNA-BD-tag in yeast cells, *TRP1*, c-Myc epitope tag	Köbler *et al.*,[10]
pGBKT7-BD-*kaiC1*	Expression of KaiC1 with an N-terminal GAL4(1–147) DNA-BD-tag in yeast cells, *TRP1*, c-Myc epitope tag	Wiegard *et al.,*[9]
pCGAD-*kaiC2*-AD	Expression of KaiC2 with a C-terminal *GAL4*(768–881) AD-tag in yeast cells, *LEU2*, HA epitope tag	This study
pGAD-AD-*kaiC2*	Expression of KaiC2 with an N-terminal *GAL4*(768–881) AD-tag in yeast cells, *LEU2*, HA epitope tag	This study
pD153-*kaiC2*-BD	Expression of KaiC2 with a C-terminal GAL4$_{(1–147)}$ DNA-BD-tag in yeast cells, *TRP1*, c-Myc epitope tag	Köbler *et al.*,[10]
pGBKT7-BD-*kaiC2*	Expression of KaiC2 with an N-terminal GAL4(1–147) DNA-BD-tag in yeast cells, *TRP1*, c-Myc epitope tag	This study
pET22-*sll0485*-his6	Expression of Sll0485 with a C-terminal His6 tag in *E. coli* cells	This study
pASK-*kaiC3*	Expression of KaiC3 with an N-terminal Strep-tag (1-11) in *E. coli* cells	Wiegard *et al.,*[9]
pGEX-*kaiB3*	Expression of KaiB3 with an N-terminal GST-tag (1-231) in *E. coli* cells	Wiegard *et al.,*[9]
pGEX-*kaiB1*	Expression of KaiB1 with an N-terminal GST-tag (1-231) in *E. coli* cells	Wiegard *et al.*,[9]
pGEX-*kaiA*7942	Expression of KaiA from *Synechococcus elongatus* PCC 7942 with an N-terminal GST-tag (1-231) in *E. coli* cells	Nishiwaki *et al.*,[11]

pUC19	Cloning vector backbone with multiple cloning site, Amp^R	Norrander *et al.,*[12]
pUC4k	Cloning vector backbone with multiple cloning site, Km^R, Amp^R	Taylor and Rose,[13]
pUC19-Δ*sll0485*	Construction of the Δ*kaiA3* strain via homologous recombination	This study
pUC19-Δ*sll0485*-compl	Construction of the Δ*kaiA3/kaiA3* complementation strain via homologous recombination	This study
pUC19-Δ*kaiA3B3*	Construction of the Δ*kaiA3B3C3* strain via homologous recombination	This study
pUR-N-Flag-xyz	pVZ321-based conjugative expression vector, expression of N-terminal FLAG-tagged genes from the copper repressible PpetJ promotor	Savakis *et al*.,[14]
pUR-NFLAG-*sll0485*	Expression of N-terminal FLAG-tagged *kaiA3.*	This study

178

Dataset S1 (separate Excel file). Putative orthologs of KaiA3 in cyanobacteria and prokaryotes. Header names are described in the following and the exact name is mentioned in parenthesis. Information is provided about the organism (name), the corresponding genus (genus), the taxonomy (taxonomy), and the taxonomic identifier (taxid). Furthermore, the annotated protein name on NCBI (protein), the protein identifier on NCBI (protein_id), the genome identifier where the protein originated from (genome_id), the date when it was last modified on NCBI (date), BLAST statistics (e_value, bitscore, identity), the length of the protein (length) as well as the sequence (seq) were recorded. In addition, the protein id of backward best hit from *Synechocystis* (synechocystis_prot_id) as well as the genome identifier for the genome assembly (synechocystis_id) was stored.

Dataset S2 (separate Excel file). Dataset from immunoprecipitation-coupled LC-MS/MS analyses of KaiC3 and KaiC1 interactome analyses. Identified and quantified proteins from label-free analysis of α-FLAG-KaiC3 or -KaiC1 and control co-immunoprecipitation are listed.

Dataset S3 (separate Excel file). Dataset of KaiA3B3C3 *in vitro* co-incubation assays on KaiC3 phosphorylation. Localized KaiC3 phosphorylation sites and phosphorylation occupancies of Ser423/Thr424 are listed.

References

1. Waterhouse AM, Procter JB, Martin DMA, Clamp M, Barton GJ. Jalview Version 2-A multiple sequence alignment editor and analysis workbench. *Bioinformatics* **25**, 1189-1191 (2009).

2. Katoh K, Standley DM. MAFFT multiple sequence alignment software version 7: Improvements in performance and usability. *Molecular Biology and Evolution* **30**, 772-780 (2013).

3. Madeira F*, et al.* The EMBL-EBI search and sequence analysis tools APIs in 2019. *Nucleic Acids Research* **47**, W636-W641 (2019).

4. Ye S, Vakonakis I, Ioerger TR, LiWang AC, Sacchettini JC. Crystal structure of circadian clock protein KaiA from *Synechococcus elongatus*. *Journal of Biological Chemistry* **279**, 20511-20518 (2004).

5. Zimmermann L*, et al.* A Completely Reimplemented MPI Bioinformatics Toolkit with a New HHpred Server at its Core. *Journal of Molecular Biology* **430**, 227-2243 (2018).

6. Rausenberger J*, et al.* Photoconversion and Nuclear Trafficking Cycles Determine Phytochrome A's Response Profile to Far-Red Light. *Cell* **146**, 813-825 (2011).

7. Hiltbrunner A*, et al.* Nuclear Accumulation of the Phytochrome A Photoreceptor Requires FHY1. *Current Biology* **15**, 2125-2130 (2005).

8. Shimizu-Sato S, Huq E, Tepperman JM, Quail PH. A light-switchable gene promoter system. *Nature Biotechnology* **20**, 1041-1044 (2002).

9. Wiegard A*, et al. Synechocystis* KaiC3 displays temperature- And KaiB-dependent ATPase activity and is important for growth in darkness. *J Bacteriol* **202**, 1-36 (2020).

10. Köbler C, Schultz SJ, Kopp D, Voigt K, Wilde A. The role of the *Synechocystis* sp. PCC 6803 homolog of the circadian clock output regulator RpaA in day–night transitions. *Molecular Microbiology* **110**, 847-861 (2018).

11. Nishiwaki T*, et al.* Role of KaiC phosphorylation in the circadian clock system of Synechococcus elongatus PCC 7942. *Proc Natl Acad Sci U S A* **101**, 13927-13932 (2004).

12. Norrander J, Kempe T, Messing J. Construction of improved M13 vectors using oligodeoxynucleotide-directed mutagenesis. *Gene* **26**, 101-106 (1983).

13. Taylor LA, Rose RE. A correction in the nucleotide sequence of the Tn9O3 kanamycin resistance determinant in pUC4K. *Nucleic Acids Research* **16**, 358 (1988).

14. Savakis P*, et al.* Light-induced alteration of c-di-GMP level controls motility of *Synechocystis* sp. PCC 6803. *Molecular Microbiology* **85**, 239-251 (2012).